Scale-invariant hidden local symmetry, topology change, and dense baryonic matter

Won-Gi Paeng,[1,*] Thomas T. S. Kuo,[2,†] Hyun Kyu Lee,[3,‡] and Mannque Rho[4,§]

[1]*Rare Isotope Science Project, Institute for Basic Science, Daejeon 305-811, Korea*
[2]*Department of Physics and Astronomy, Stony Brook University, Stony Brook, New York 11794, USA*
[3]*Department of Physics, Hanyang University, Seoul 133-791, Korea*
[4]*Institut de Physique Théorique, CEA Saclay, 91191 Gif-sur-Yvette cédex, France*

When scale symmetry is implemented into hidden local symmetry in low-energy strong interactions to arrive at a scale-invariant hidden local symmetric (HLS) theory, the scalar $f_0(500)$ may be interpreted as pseudo-Nambu-Goldstone (pNG) boson, i.e., dilaton, of spontaneously broken scale invariance, joining the pseudoscalar pNG bosons π and the matter fields $V = (\rho, \omega)$ as relevant degrees of freedom. Implementing the skyrmion–half-skyrmion transition predicted at large N_c in QCD at a density roughly twice the nuclear matter density found in the crystal simulation of dense skyrmion matter, we determine the intrinsically density-dependent "bare parameters" of the scale-invariant HLS Lagrangian matched to QCD at a matching scale Λ_M. The resulting effective Lagrangian, with the parameters scaling with the density of the system, is applied to nuclear matter and dense baryonic matter relevant to massive compact stars by means of the double-decimation renormalization-group $V_{\mathrm{low}\,k}$ formalism. We satisfactorily postdict the properties of normal nuclear matter and more significantly *predict* the equation of state of dense compact-star matter that quantitatively accounts for the presently available data coming from both the terrestrial and space laboratories. We interpret the resulting structure of compact-star matter as revealing how the combination of hidden-scale symmetry and hidden local symmetry manifests itself in compressed baryonic matter.

I. INTRODUCTION

In a preceding note [1], the notion that the $f_0(500)$, the lowest scalar listed in the particle data booklet, is a dilaton arising from the spontaneous breaking of scale invariance in QCD [2] was implemented into hidden local symmetry (HLS) [3] of the light-quark vector mesons $V_\mu = (\rho_\mu, \omega_\mu)$ that embodies the nonlinear realization of chiral symmetry into a scale-invariant hidden local symmetry theory (*s*HLS for short) and the resulting Lagrangian was subjected to the vacuum change due to the density of baryonic matter.

In this paper, we confront the resulting formalism with what's known of normal nuclear matter and make predictions on properties of dense matter appropriate for massive compact stars.

Since the basic premise for the effective Lagrangian that we shall employ, *s*HLS, is fully expounded in Ref. [1], we shall eschew details and limit ourselves here only to what are essential for the calculations that we make. We shall follow closely the procedures given in Ref. [1]. The only issue that was not given an adequate comment in Ref. [1] is the place of an infrared (IR) fixed point postulated in Ref. [2] in QCD with the number of flavors $N_f \sim 3$ as needed in nuclear phenomena. It is perhaps worth making a brief remark on it. It is argued in Ref. [2] that the notion that QCD has an

IR fixed point for $N_f = 3$ with the resulting "scale-chiral symmetry" solves some of the long-standing puzzles in particle physics that involve "light" scalar excitations. For instance, phrased in terms of a scale-chiral counting rule generalizing the chiral counting rule of chiral perturbation theory, it gives a surprisingly simple explanation of the $\Delta I = 1/2$ rule, accounts for the mass and width of the scalar $f_0(500)$, etc. As stressed in Ref. [1], it could also resolve long-standing conundrums in nuclear physics involving a low-mass scalar. Unfortunately, however, there is, so far, no convincing proof that the three-flavor QCD has an IR fixed point: Neither lattice nor model-independent approaches have uncovered it. This is in contrast to QCD at $N_f \sim 8$ being studied for the dilatonic Higgs model for going beyond the Standard Model (for a recent summary, see [4]). This does not imply that an IR fixed point advocated in Ref. [2] is ruled out. As argued in Ref. [2], an IR fixed point at which scale-chiral symmetry is realized in the Nambu-Goldstone mode has not yet been probed by the lattice work.

In this paper, we take the point of view that in dense matter, the scale-chiral symmetry of the sort advocated by [2] could be present as an "emergent symmetry." This is in some sense similar to hidden local symmetry which plays an equally important role in our calculation. The notion of hidden local symmetry which gives the famous "VD (vector dominance)" and Kawarabayashi-Suzuki-Riazuddin-Fayyazuddin (KSRF) relation makes sense only if the vector meson V_μ is light. There are two known cases where the "lightness" of V_μ is realized. One is the presence of the vector manifestation (VM) fixed point at which the vector meson mass goes to zero as does the pion mass (in the chiral limit) [3]. The other is supersymmetric

―――――――
*wgpaeng@ibs.re.kr
†kuo@tonic.physics.sunysb.edu
‡hyunkyu@hanyang.ac.kr
§mannque.rho@cea.fr

QCD in certain parameter space [5]. In what follows, the VM fixed point, emerging at high density, will play a key role. In a similar vein, a scalar of ∼600 MeV fluctuating around an IR fixed point will figure crucially in the equation of state (EoS) for dense matter.

It is rather intriguing that the two symmetries we are combining, i.e., scalar symmetry and (vector) local symmetry, are hidden in baryonic matter (as in the beyond-the-Standard-Model regime [4]) and seem to emerge at high density.

II. SCALE-INVARIANT HLS LAGRANGIAN

The Lagrangian we will consider, sHLS, simplified from [1], takes the form

$$\mathcal{L}_{s\text{HLS}}(U, \chi, V_\mu)$$

$$\approx \mathcal{L}_{\text{HLS}}^{(2)}\left(\frac{\chi}{f_{0\sigma}}\right)^2 + \frac{f_{0\pi}^2}{4}\left(\frac{\chi}{f_{0\sigma}}\right)^3 \text{Tr}(MU^\dagger + \text{H.c.}) + \cdots$$

$$+ \frac{1}{2}\partial_\mu\chi\partial^\mu\chi + V(\chi), \tag{1}$$

where $\chi = f_\sigma e^{\sigma/f_\sigma}$ is the "conformal compensator" field with σ the nonlinear dilaton field and $f_\sigma = \langle\chi\rangle$ the vacuum expectation value (VEV) (either matter-free or in-medium), the chiral field U consists of (L, R) fields as $U = e^{i2\pi/f_\pi} = \xi_L^\dagger \xi_R$ with $\pi = \frac{1}{2}\vec{\tau}\cdot\vec{\pi}$, M is the quark-mass matrix representing chiral symmetry breaking which also breaks scale symmetry, $f_{0\sigma}$ is the medium-free-vacuum expectation value $\langle 0|\chi|0\rangle$ and $V(\chi)$ is the dilaton potential that encodes the spontaneous and explicit breaking of scale invariance. For simplicity, the HLS Lagrangian is given to $\mathcal{O}(p^2)$, with the ellipsis standing for higher scale–chiral order terms. Note that we are taking the approximation $c_i \approx 1$ in the notation of Ref. [2]. The potential $V(\chi)$ contains several unknown constants in Ref. [2] of which we do not need their specific forms for our analysis.

A. Intrinsic density dependence (IDD) of "bare" parameters of sHLS

In order to confront the Lagrangian (1) with nuclear matter and high density matter, there are three indispensable ingredients to consider. First, the baryon degrees of freedom have to be incorporated. Second, the "bare" parameters of the effective Lagrangian need to be matched to QCD. Third, strong correlations between nucleons, including possible phase changes, have to be included as one goes up in density.

All three could in principle be handled—at least in some approximations such as large N_c—using skyrmion description of baryons and baryonic matter [1]. Some progress has been made in this direction [6] but the mathematics required is still too daunting to arrive at a reliable result. We shall therefore put baryons explicitly "by hand" in a scale-chiral symmetric way. Let us call the baryon-field-implemented Lagrangian bsHLS for short. Since high density, $n \sim (5$–$7)n_0$ (where n_0 is the nuclear matter density), going toward chiral transition is involved, the "bare" parameters need to have contact with QCD parameters. This will be done by matching the correlators of the bsHLS Lagrangian to those of QCD at an appropriate

matching point Λ_M lying below the chiral scale $\Lambda_\chi \sim 1$ GeV, say, at about the ρ mass. It is important to note that the matching endows the "bare" parameters of EFT Lagrangian with dependence on the quark condensate $\langle\bar{q}q\rangle$, the gluon condensate $\langle G^2\rangle$, etc. Since those condensates depend on the "vacuum," they will of course depend on density which modifies the vacuum if the EFT Lagrangian is embedded into a medium. The crucially important point in our development is that *the density dependence involved here is intrinsic of QCD, to be distinguished from the density dependence coming from (mundane) nuclear many-body correlations.* This density dependence—that will play a key role in what follows—will be referred to, as in Ref. [1], as "intrinsic density dependence" (IDD for short).

B. Double-decimation RG procedure

Now given the effective field theory (EFT) Lagrangian endowed with the IDDs, nuclear dynamics is treated by renormalization-group (RG) decimation from the matching scale Λ_M down to the appropriate low-energy scale where the processes we are interested in take place. For this, a highly versatile tool is the $V_{\text{low }k}$ strategy [7,8]. We will exploit it in this paper. A convenient—and successful—procedure in nuclear physics is the "double decimation" RG flow described in Ref. [9]. In fact, this procedure was used for the first time for the EoS for massive stars in Ref. [10]. In this paper, we will improve on it both in concept and in numerics, assuring consistency with the scale-chiral symmetry adopted in Ref. [1].

In the $V_{\text{low }k}$ framework, the double decimation consists of the first step from Λ_M to the scale at which $V_{\text{low }k}$ is obtained. The second step is to decimate to the Fermi sea around which fluctuations are computed to take into account multibody correlations. This is equivalent to fluctuating around the Landau Fermi-liquid fixed point [11]. It is in doing these decimation calculations using $V_{\text{low }k}$ that information from a topology change encoded in the skyrmion crystal treatment of dense matter enters. This transition involves no local order-parameter field and hence may not belong to the Ginzburg-Landau-Wilson paradigm but as will be seen, has a drastic impact on the EoS in compact-star matter. While the topology change that takes place in the skyrmion crystal is, strictly speaking, valid only in the large N_c limit of QCD, it seems quite universal, visible already in the structure of the α particle with four nucleons [12,13]. It is thus highly plausible that such a half-skyrmion topological structure could be present in dense matter, say, above nuclear matter density. What is done in this paper is that this feature of changeover from skyrmions to half skyrmions in the soliton description is translated into the bare parameters of the effective Lagrangian, in terms of changes in IDDs. It effectively demarcates the EFT Lagrangian into two density regimes, one for (I) $n \lesssim n_{1/2}$ and the other for (II) $n \gtrsim n_{1/2}$. The former (I) entails the "bare" parameters of the Lagrangian that carry the density dependence referred to as "IDD$_{\text{pNG}}$" where the pseudo-Nambu-Goldstone [(pseudo-)NG] bosons figure and the latter (II) "IDD$_{\text{matter}}$" in which the matter fields V_μ intervene. An interesting observation made in Higgs physics [4] where also both hidden scale symmetry and hidden local symmetry enter is that

the properties of (techni)vector mesons are scale invariant. Intriguingly, it turns out also in dense matter that the ρ meson properties are scale invariant, controlled by the VM fixed-point structure.

III. SYMMETRY ENERGY, TENSOR FORCES, AND TOPOLOGY

One of the most interesting observables in dense matter is the "symmetry energy factor" S defined in the energy E per particle of nucleus consisting of P protons and N neutrons, i.e., $A = P + N$,

$$E(n,x) = E_0(n,0) + S(n)x^2 + \cdots , \qquad (2)$$

with $x = (N - P)/A$. Here n stands for the baryon number density and the ellipsis stands for higher-power terms in x. The quadratic approximation is known to be reliable, so we focus on S. As is well known, the symmetry energy is the quantity, representing neutron excess of the system, that plays a key role in the EoS of compact stars. It is this quantity that is strongly influenced by topology in the skyrmion picture, manifested through the nuclear tensor forces.

As mentioned above, a robust feature of skyrmion description of nucleonic matter—that we shall exploit in what follows—is that there is a "changeover" from a state of skyrmions to a state of half skrymions at some matter density denoted $n_{1/2}$. Its presence in the skyrmion framework is remarkably independent of the degrees of freedom involved and is quite insensitive to the parameters of the Lagrangian. It is present in the Skyrme model with pions only as well as in sHLS models with the vectors and/or the dilaton [12]. Precisely at which density the changeover takes place is, however, model dependent and cannot be pinned down precisely in the present state of formulation. However the density at which the half-skyrmion appears, $n_{1/2}$, is found to be insensitive to the dilaton mass, the most uncertain quantity in the calculation. This feature is seen in the model in which skyrmions are put on crystal lattice [6,14]. In what follows, *our basic premise will be that in terms of the skyrmion picture justified at high density and for large N_c, half skyrmions could appear at some density in the vicinity of $\sim 2n_0$.* What ensues is a striking consequence on the symmetry energy.

Since the phenomenon considered is quite generic, more or less independent of the degrees of freedom involved, we can address the matter using the simplest model, i.e., the Skyrme model [15] that consists of two terms, the current algebra term and the Skyrme quartic term implemented with the conformal compensator field. It corresponds to dropping the vector meson fields and putting the Skyrme quartic term—which is of scale dimension 4 and hence scale invariant—in place of the ellipsis in Eq. (1). We expect the result to be qualitatively the same with the more realistic Lagrangian (1).

With skyrmions put on crystal, the easiest way to compute the symmetry energy is to rotationally quantize A-neutron skyrmion matter, which corresponds to calculating S from (2) for $x = 1$ [16]. It is given by

$$S \approx \frac{1}{8\lambda_I} . \qquad (3)$$

Here λ_I is the isospin moment of inertia of $\mathcal{O}(N_c)$ given by the space integral over the single cell of the hedgehog configuration U_0 and the dilaton configuration. In the presence of vector mesons, the integral will also involve the mesons's classical configurations. It is of the leading order in N_c, with fluctuation corrections suppressed by $1/N_c$.

The striking feature of the symmetry energy factor (3) turns out to be a cusp structure at the changeover density $n_{1/2}$—which comes out at $n_{1/2} \sim (1.3$–$2.0)n_0$. The numerical calculation of Eq. (3) reveals that the S decreases monotonically as density increases toward $n_{1/2}$ and then turns up and monotonically increases after $n_{1/2}$.

Now it may be that the method anchored on crystal is not applicable to low-density matter. Furthermore nuclear matter at equilibrium density is known to be in Fermi liquid. Therefore one might object to applying the crystal skyrmion description not too far above the nuclear matter density. However it turns out that the cusp structure at a density at $\sim 2n_0$ is not an artifact of crystal background and can be trusted. In fact what is highly nontrivial is that this feature can be easily reproduced by the microscopic structure of the tensor forces, in particular, the effect on the tensor forces of the topological change at $n_{1/2}$. For this, we use the fact that the symmetry energy is dominated by the tensor forces [17]. We first write the effective Lagrangian (1) that implements the topology change at $n_{1/2}$ in the skyrmion description. To do this, we divide the density regime into two regions—R(egions) I and II—with the demarcation at $n_{1/2}$,

$$\text{R(egion) I} : 0 < n < n_{1/2}, \qquad (4)$$

$$\text{R(egion) II} : n_{1/2} \leqslant n \leqslant n_c . \qquad (5)$$

As described in Ref. [1], we can translate the topology change into scaling (that is, IDD) properties of the parameters of the Lagrangian (1) in the two regions. The principal parameters involved are the decay constants $f_{\pi,\sigma}$ and masses $m_{\pi,\sigma}$ of the pseudo-Nambu-Goldstone bosons, the coupling constants $g_{\rho,\omega}$ and masses $m_{\rho,\omega}$ of the hidden gauge fields, etc. The specific parametrization that we extract from the strategy detailed in Ref. [1] will be used for the $V_{\text{low}\,k}$ approach presented in Sec. V and is described in the next section. Here we make use of it in showing how the cusp in S can be understood in the given framework. In this approach, one first constructs nuclear potentials in terms of the exchange of the meson degrees of freedom given in the Lagrangian with the scaling parameters. Apart from the IDDs in the Lagrangian, this is essentially what is done in nuclear chiral perturbation theory. Now in terms of our sHLS Lagrangian, the tensor forces V_T consist of π and ρ exchanges, $V_T = V_T^\pi + V_T^\rho$. The notable feature of $V_T^{\pi,\rho}$ is that the two contributions, having the same radial form with different masses, come with the opposite sign. Thus the net tensor force involves a crucially important cancellation between the two components, which depends on the scaling properties of the two components. As will be seen in the next section, the details are a bit involved, but the qualitative feature is simple.

As noted, the prominent feature of the net tensor force at $n_{1/2}$ is the abrupt change in the slope. In R-I, the pion tensor

is almost completely unaffected by density within the range of
density we are considering, due to what one might interpret as
the protection by chiral symmetry. This has been numerically
confirmed up to $\simeq 5n_0$; see Appendix A. The ρ tensor, on
the other hand, gets enhanced as density increases due to the
dropping of its mass. Since it comes with the sign opposite
to the pion tensor, it cancels part of the pionic tensor. The
net effect is then that the tensor force becomes weaker as
density increases. This tendency is in agreement with a variety
of observations in nuclei, the most spectacular of which is
the long lifetime for carbon-14 [18], i.e., the C-14 dating.
(It should be mentioned that short-range three-body forces,
present as contact interaction in chiral perturbation theory,
could do the same suppression of the Gamow-Teller matrix
element involved. As explained in Ref. [19], however, this does
not represent a different mechanism to that of [18]. It may be
said that most, if not all, of the effect of the contact three-
body forces, largely responsible for the suppression of the
Gamow-Teller matrix element, is encoded in the IDD included
in Ref. [18].) The weakening of the net tensor force continues
up to the changeover density $n_{1/2}$. At $n_{1/2}$, the tensor force
stops decreasing, turns over and starts increasing, with the
pion tensor becoming dominant. There are two mechanisms
at work here. One is that the change of parameters that takes
place at $n_{1/2}$ strongly suppresses the overall strength of the
ρ tensor force although the mass continues dropping. The
other is that in R-II, the candidate order parameter for chiral
symmetry is a four-quark condensate with the bilinear quark
condensate suppressed (it goes to zero at $n_{1/2}$ in the skyrmion
crystal). And the four-quark condensate is found to be strongly
suppressed in Region II [6]. Interpreted in terms of a Gell-
Mann-Oakes-Renner (GMOR) relation for in-medium pion,
this would imply, since the in-medium decay constant remains
more or less unscaling in density in R-II, that the pion mass
must then decrease. As a consequence, the pion tensor must
become stronger, even further enhanced over and above the
free-space value. This will facilitate pion condensation, as
expected at high density in crystal form. Given the abrupt
change in the tensor force at $n_{1/2}$, the cusp structure in the
symmetry energy found in the skymion model follows in an
immediate way as explained below.

In summary, there is a change in the slope of the symmetry
energy factor S at $n_{1/2}$, a semiclassical result (in the sense of
large N_c effect) which is a robust feature in the framework
of sHLS theory. How it manifests in nature requires a
sophisticated treatment of many-body theory. What follows
in this paper is a detailed analysis of this feature in the RG-
implemented $V_{\mathrm{low}\,k}$ approach which takes into account high-
order correlations encoded in Landau–Fermi-liquid theory.

IV. TOPOLOGICAL DEMARCATION
OF DENSITY REGIMES

A. Intrinsic density dependence (IDD)

In this section we specify the effective sHLS Lagrangian
that is endowed with the density dependence IDD inherited
from QCD at the matching scale Λ_M. As announced, we
deal with two density regimes—Regions I and II—when the

system is embedded in medium. That there can be two regimes
demarcated at a density above n_0 is neither indicated by a
general QCD argument nor by model-independent effective
field theory arguments. It is however predicted in the skyrmion
description of dense matter which is strictly valid in the
large N_c limit and at high density. We take this into account
by interpreting, as described above, the demarcation as the
changes in the density dependence of the effective Lagrangian
that is applicable to the $V_{\mathrm{low}\,k}$ approach.

The Lagrangians (6) and (22) applicable in R-I and R-II,
respectively, are written in Lorentz-invariant form. One may
object to their form saying that they should actually take
O(3) covariant form in medium since the Lorentz symmetry
is spontaneously broken. In fact the O(3) covariant HLS La-
grangian was written down before [20]. However in the scheme
we are using with the correlators, the density dependence of
the bare parameters of the Lagrangian is in "vacuum-specific
condensates." These do not intervene in spontaneous breaking
of Lorentz symmetry [21]. The symmetry breaking that breaks
the O(4) symmetry comes in RG decimations *à la* $V_{\mathrm{low}\,k}$ with
the given Lagrangians. Furthermore in the hidden-scale-HLS
framework, as density goes above $n_{1/2}$, the quark condensate,
while supporting chiral density wave, goes to zero on average
and the vector mass drops rapidly toward the VM fixed
point. When these two phenomena take place, the Lorentz
symmetry breaking decreases surprisingly rapidly [20]. Thus
the pion velocity, for instance, approaches 1 quickly. We
should point out that the situation is totally different in the
absence of the vector meson with the VM fixed point [22].
The relativistic mean field approach with the Lagrangian
with density-dependent parameters, popularly used in nuclear
theory circles, is justified along this line of reasoning at high
density.

1. Region I

Consider first Region I (4). This is the normal nuclear
matter phase, extrapolated to density $n_{1/2}$ which can be de-
scribed in a multitude of phenomenologically reliable models.
Currently most popular is the chiral perturbative approach,
i.e., two-flavor $\chi\mathrm{PT}_2$. The $V_{\mathrm{low}\,k}$ approach can be considered
as an improved version of $\chi\mathrm{PT}_2$, in that one universal IDD
intervenes and improves on the phenomenology in the vicinity
of nuclear matter where data are available.

To be specific while preserving simplicity, we write the
in-medium "bare" bsHLS Lagrangian in a linearized form

$$\mathcal{L}_I = \overline{N}[i\gamma_\mu(\partial^\mu + igV^\mu) - m_N^* + g_\sigma\sigma]N - \frac{1}{4}V_{\mu\nu}^2$$
$$+ \frac{m_V^{*\,2}}{2}V^2 + \frac{1}{2}(\partial_\mu\sigma)^2 - \frac{m_\sigma^{*\,2}}{2}\sigma^2 + \frac{1}{2}\partial^\mu\vec{\pi}\cdot\partial_\mu\vec{\pi}$$
$$- \frac{1}{2}m_\pi^{*\,2}\vec{\pi}^2 + \mathcal{L}_{\pi m} + \cdots, \tag{6}$$

where the ellipsis stands for possible terms that are of higher
order in chiral-scale counting and of higher fields and $V_\mu =
\vec{\tau}\cdot\vec{\rho}_\mu + \omega_\mu$ assumed to be flavor-U(2) symmetric. Since the
flavor U(2) symmetry for the vectors V_μ seems to be fairly
good in the matter-free vacuum, it should hold also in low-
density regime, i.e., R-I. (At high density in R-II, however,

we will find that the U(2) symmetry must break down [23].) $\mathcal{L}_{\pi m}$ stands for the pion-matter and pion-σ couplings. The matching of the EFT Lagrangian to QCD renders the pion decay constant f_π and the dilaton decay constant f_σ dependent on the QCD condensates $\mathcal{C}$, i.e., $\langle \bar{q}q \rangle, \langle G^2 \rangle$, etc. Since the condensates reflect the vacuum structure, in medium, the decay constants depend on density, which will be denoted with an asterisk, $f_{\pi,\sigma}^*$. As stated, *this density dependence is an intrinsic property of the QCD vacuum structure, to be distinguished from density dependence that is due to standard nuclear many-body correlations.* This distinction arises from the strategy of matching EFT to QCD.

Following the reasoning given in Ref. [1], we can relate the in-medium decay constants as

$$f_\pi^*/f_{0\pi} \approx f_\sigma^*/f_{0\sigma} \equiv \Phi_I(n), \tag{7}$$

where $f_{0\pi,\sigma}$ are the decay constants in the matter-free vacuum.[1] This follows from the nature of Nambu-Goldstone bosons reflecting the locking of the chiral symmetry to the scale symmetry, that is, $\mathrm{IDD_{pNG}}$. The pion and dilaton decay constants depend on QCD condensates $\mathcal{C}$, the former on the quark condensate *à la* GMOR and the latter on both the quark condensate and gluon condensate [1,2]. Since there is no lattice calculation in dense medium, the scaling function Φ is not really known from QCD proper. For low density, one may resort to chiral perturbation theory $\chi\mathrm{PT}_2$. More pertinently—and fortunately—there is information from experiments where the pion decay constant is measured up to n_0, e.g., in the deeply bound pionic system. One immediate consequence of $\mathrm{IDD_{pNG}}$ is the d(ensity)-scaling of the pion mass

$$m_\pi^*/m_\pi \approx \Phi_I^{1/2}. \tag{8}$$

How the dilaton mass d-scales is more complicated. We will return to it later.

As for the properties of, and coupling, to the matter fields, one needs to consider the $\mathrm{IDD_{matter}}$, that is, due to the matching of the vector and axial vector correlators. However as argued in Ref. [1] and elsewhere based on phenomenology, to the order we are considering, the $\mathrm{IDD_{matter}}$ can be ignored in R-I, so we can focus only on $\mathrm{IDD_{pNG}}$ effects.[2] This yields

$$m_N^*/m_N \approx m_V^*/m_V \equiv \Phi_I. \tag{9}$$

To the same approximation, the hidden gauge coupling g and the σNN coupling g_σ do not d-scale,

$$g^*/g \approx g_\sigma^*/g_\sigma \approx 1. \tag{10}$$

On the contrary, the pion-NN coupling in $g_{\pi NN}(\bar{N} \frac{1}{2} \vec{\tau} \cdot \vec{\pi} \gamma_5)N$ d-scales,[3]

$$g_{\pi NN}^*/g_{\pi NN} \approx \Phi_I. \tag{11}$$

This implies, by the low-energy theorem known as Goldberger-Treiman relation,

$$g_A^*/g_A \approx \Phi_I. \tag{12}$$

Finally we turn to the dilaton mass m_σ^*. As discussed at length in Ref. [1], the dialton being a pseudo-Goldstone scalar with explicit scale-symmetry breaking due to an intricate interplay, un-understood yet, of the trace anomaly and the current quark mass, we are unable to determine with confidence the d-scaling of the dilaton mass with the dilaton potential of [2]. If however one took the dilaton potential of the Coleman-Weinberg-type log potential just to have an idea, one would obtain

$$m_\sigma^*/m_\sigma \approx \Phi_I. \tag{13}$$

In R-I, a reasonable parametrization that we shall use is

$$\Phi_I(n) \approx \frac{1}{1 + c_I\, n/n_0}. \tag{14}$$

The value of $c_I > 0$ used in numerical analysis will be given in Sec. VI.

Though not highly rigorous, this is supported up to nuclear matter density [25] by IDD-implemented Walecka-type mean field, so we will assume it in the numerical analysis given below. This completely determines the bare Lagrangian (6). Only one d-scaling function Φ_I is to be determined and this can be done by resorting to pionic nuclear systems and/or chiral perturbation theory. For quantitatively accurate agreement with Nature, however, a small fine-tuning on c_I will be required in Sec. VI.

2. Region II

In this region, there is no guidance either from experimental data or from trustful theory—except for the hidden local symmetry prediction given below in Eq. (15). This makes a precise determination of the effective Lagrangian problematic. Thus our approach is highly exploratory and uncertain. What is clear is that the density dependence of the parameters must undergo drastic modifications as the system goes across the changeover point $n_{1/2}$: First chiral perturbation theory, formulated to work well up to nuclear matter density, most

---

[1] Given the "$c \approx 1$ approximation" made in locking chiral symmetry to scale symmetry [1], we use approximate equality instead of equality.

[2] The matching of the vector and axial vector correlators does make the pion decay constant f_π inherit the quark and gluon condensates from QCD but their effects are negligible. It cannot account for vanishing pion decay constant as the quark condensate is dialled to zero. It requires a subtle role of quadratic divergence in the pion loops in RG decimation. Furthermore f_σ—that locks scale symmetry to chiral symmetry—cannot enter into the correlators of the isovector currents we have for $\mathrm{IDD_{matter}}$. On the contrary, we will see later the situation is entirely different in Region II.

[3] It should be noted that the conformal compensator trick used in this paper works differently between the linear π-nucleon coupling which is used for (11) and the nonlinear coupling that figures in the bsHLS Lagrangian. In the latter, the axial coupling constant g_A will not d-scale and hence neither will $g_{\pi NN}$. This has to do with a well-known problem of the so-called "quenching of g_A in nuclei" that comes from the role of the Δ resonance in the baryon sector. The g_A obtained in the linear coupling accounts for the role of the Δ that is integrated out from the bsHLS Lagrangian. This is an old story that dates back to 1974 with the quenching of g_A by a Δ-hole mechanism. See, e.g., [24]. In this paper we will use this scaling which is not properly included in the $\mathrm{IDD_{pNG}}$ but is required for consistency.

likely breaks down at some high density in Region II. This is because chiral perturbation theory makes sense in small-k_F expansion whereas the Fermi-liquid fixed point approach relies on small $1/k_F$ expansion [26]. Second the local U(2) symmetry assumed in R-I is likely to break down. Third, most significantly, in hidden local symmetry for the ρ meson which would be more justified as the vector-meson mass drops to the level of pNG bosons, there is the vector manifestation (VM) of hidden local symmetry, at the approach to which the mass d-scale to zero as

$$m_\rho \sim g_\rho \sim \langle \bar{q}q \rangle \to 0 \tag{15}$$

as $\langle \bar{q}q \rangle \to 0$, where we define g_ρ as the hidden local gauge coupling for ρ to distinguish it from g_ω for ω. What is significant in this behavior is that it is the hidden gauge coupling g_ρ—which is un-scaling in R-I unaffected by IDD$_{pNG}$—that plays an important role. Similarly the pion decay constant vanishing only very near the density at which chiral symmetry is restored, hence in R-II approaching the density that drives the system to the VM fixed point, is intricately connected to the matching process [3]. This means that IDD$_{matter}$ must become operative in R-II; (1) from a phenomenological point of view, were the parameters of Region I to continue to higher density much above n_0, then the symmetry energy factor would become "supersoft" at a density $n \gtrsim (3-4)n_0$ which would require modification to gravity theory [27].

There is also a possibility that the Fermi-liquid structure, assumed to hold in R-I, breaks down in R-II. This possibility will not be considered in this paper.

To account for a rapid changeover at $n_{1/2}$ in sHLS, we take the d-scaling for the ρ vector meson in R-II to be consistent with the VM

$$m_\rho^*/m_\rho \propto g_\rho^*/g_\rho \equiv \Phi_{II}^\rho. \tag{16}$$

Approaching the VM fixed point, we take the linear density scaling

$$\Phi_{II}^\rho(n) \approx \left(1 - c_{II}^\rho n/n_0\right) \tag{17}$$

with c_{II}^ρ will be fixed to give the chiral restoration density, for rough estimate, $n_c \sim (6\text{–}7)n_0$.

The density $n_{1/2} \sim 2n_0$ may be a bit too far from the VM fixed point for this d-scaling (16) to be quantitatively accurate, but one can take this as expanding around the VM fixed point as was done for kaon condensation that takes place at $n \sim 3n_0$ [28]. An approximately same critical density—near $n_{1/2}$—is arrived at by expanding around equilibrium nuclear matter treated as the Fermi-liquid fixed point [25].

If the local U(2) symmetry for (ρ, ω) were good in R-II as it seems to be in R-I, one could use the same reasoning given above for ρ. However there is nothing to indicate that the symmetry would hold there. For instance, the reasoning that goes into the VM fixed point for the ρ based on correlators as given in Ref. [3] does not apply to the ω meson. In fact if one assumes U(2) symmetry and let the ω behave in the same way as the ρ in R-II with the VM property (17), both symmetric nuclear matter and neutron matter become unstable just above the demarcation density $n_{1/2}$. This feature, shown in Appendix C, is the first clear message *within the framework developed in this paper* that U(2) symmetry could be badly broken at high density. We shall therefore relinquish the U(2) hidden local symmetry for the vector mesons and treat the ρ in SU(2) HLS and the ω in U(1) HLS as in Ref. [23].

The ω mass formula takes the same Higgsed mass as that of ρ,

$$m_\omega^2 = f_\omega^2 g_\omega^2, \tag{18}$$

where $m_\rho^2 = f_\rho^2 g_\rho^2$ and f_ω is the U(1) analog to $f_\rho = \sqrt{a_\rho} f_\pi$.[4] In analogy to the case of ρ, we define a_ω as

$$f_\omega = \sqrt{a_\omega} f_\pi. \tag{19}$$

Now we do not know how m_ω scales apart from the IDD$_{pNG}$ factor f_σ^*. In fact, neither f_ω nor g_ω is known in medium.[5] In what follows in confronting Nature, we will rely on Nature to guide us in arriving at the properties of ω at high density.

For the d-scaling of other quantities, we again resort to qualitative features found in the skyrmion crystal simulation focusing on the skyrmion-half-skyrmion changeover [6]. They are as follows:

(i) In-medium nucleon mass m_N^* goes like f_π^* which is consistent with the large N_c property $m_N^* \sim e f_\pi^*$ where $e \sim \mathcal{O}(N_c^{1/2})$ is related to the scale-invariant Skyrme term in the Skyrme Lagrangian, hence non-d-scaling. Somewhat surprisingly, the pion decay constant remains roughly non-d-scaling after $n_{1/2}$ until very near the chiral restoration point. Therefore we think it reasonable to take

$$m_N^*/m_N \approx m_\sigma^*/m_\sigma \approx f_\sigma^*/f_{0\sigma} \approx f_\pi^*/f_{0\pi} \approx \kappa, \tag{20}$$

where $\kappa \leqslant 1$ is more or less non-d-scaling constant up to near the chiral restoration density at which it could drop to zero.

(ii) If one assumes that the Goldberger-Treiman-like relation with the dilaton holds, i.e., $m_N^* \approx g_\sigma^* f_\sigma^*$ [1], then it is a good approximation to take

$$g_\sigma^*/g_\sigma \approx \text{const} \approx 1. \tag{21}$$

This completes the density dependence of the Lagrangian in R-II,

$$\mathcal{L}_{II} = \overline{N}[i\gamma_\mu(\partial^\mu + ig^* V^\mu) - m_N^* + g_\sigma \sigma]N - \frac{1}{4}V_{\mu\nu}^2$$
$$+ \frac{m_V^{*2}}{2}V^2 + \frac{1}{2}(\partial_\mu \sigma)^2 - \frac{m_\sigma^{*2}}{2}\sigma^2$$
$$+ \frac{1}{2}\partial^\mu \vec{\pi} \cdot \partial_\mu \vec{\pi} - \frac{1}{2}m_\pi^{*2}\vec{\pi}^2 + \mathcal{L}_{\pi m} + \cdots \tag{22}$$

If U(2) symmetry held for the vector mesons, there would be only two parameters in Region II, the constant κ and the d-scaling factor Φ_{II}^ρ that should go to zero as the VM fixed

---

[4]Phenomenologically, a_ρ is determined to be ~ 2.1 in the matter-free space [3].

[5]Note that in the vacuum the near mass degeneracy of ρ and ω gives the hint that $g_\rho \approx g_\omega$ and $a_\rho \approx a_\omega$.

point is approached. Recall that in Region I, there is only one d-scaling function Φ_I. As shown in Appendix C, the symmetry is broken in medium in R-II, hence in Eq. (22). In this case, one expects two additional scaling parameters for the ω, i.e., g_ω^* and a_ω^*. In the analysis made below, we will see how these parameters are constrained by the EoS for compact stars.

B. Effect on the tensor forces

In this subsection, we describe the structure of the tensor forces affected by the IDDs given in the previous subsection. Here the ω meson turns out to affect little the symmetry energy factor S. To see the qualitative feature of the tensor force in medium, we use the nonrelativistic ($\frac{k^2}{m_N^{*2}} \ll 1$) form of the tensor potential, valid in the region we are considering as the in-medium nucleon mass stays heavy. The tensor potential [18,29] is given by

$$V_M^T(r) = S_M \frac{f_{NM}^{*2}}{4\pi} \tau_1 \tau_2 S_{12} \mathcal{I}(m_M^* r), \qquad (23)$$

$$\mathcal{I}(m_M^* r) \equiv m_M^* \left(\left[\frac{1}{(m_M^* r)^3} + \frac{1}{(m_M^* r)^2} + \frac{1}{3 m_M^* r} \right] e^{-m_M^* r} \right), \qquad (24)$$

where $M = \pi, \rho, S_{\rho(\pi)} = +1(-1)$ and

$$S_{12} = 3 \frac{(\vec{\sigma}_1 \cdot \vec{r})(\vec{\sigma}_2 \cdot \vec{r})}{r^2} - \vec{\sigma}_1 \cdot \vec{\sigma}_2 \qquad (25)$$

with the Pauli matrices τ^i and σ^i for the isospin and spin of the nucleons with $i = 1, 2, 3$. The strength f_{NM}^* scales as

$$R_M \equiv \frac{f_{NM}^*}{f_{NM}} \approx \frac{g_{MNN}^*}{g_{MNN}} \frac{m_N}{m_N^*} \frac{m_M^*}{m_M}, \qquad (26)$$

where g_{MNN} are the effective meson-nucleon couplings. Their relations to the coupling constants that figure in the Lagrangians will be specified below. What is significant in Eq. (23) is that given the same radial dependence, the two forces (through the pion and ρ meson exchanges) come with an opposite sign and this well-known fact plays a crucial role.

First, we discuss the d-scalings of the tensor forces in medium given by IDDs and predict how the net tensor force scales in density. For the π tensor force, applying IDD$_{\text{pNG}}$ (in R-I) and IDD$_{\text{matter}}$ (dominantly in R-II) to π and N, we have from Eqs. (9), (11), and (20)

$$R_\pi \approx \frac{g_{\pi NN}^*}{g_{\pi NN}} \frac{m_N}{m_N^*} \frac{m_\pi^*}{m_\pi} \qquad (27)$$

$$\approx \begin{cases} \Phi_I \times \Phi_I^{-1} \left(\frac{m_\pi^*}{m_\pi} \right) & \text{for R-I} \\ \kappa \times \kappa^{-1} \left(\frac{m_\pi^*}{m_\pi} \right) & \text{for R-II} \end{cases} \qquad (28)$$

hence

$$R_\pi \approx \frac{m_\pi^*}{m_\pi} \quad \text{in both R-I and R-II.} \qquad (29)$$

Thus the π-tensor force principally depends only on the d-scaling of m_π^*. It turns out as has been assumed since a long

time that the pion tensor is insensitive to density: Within R-I, to the extent that the small pseudo-NG pion mass is in some sense protected by chiral symmetry, we expect the d-scaling of R_π^2 to be small. And so will be $\mathcal{I}(m_\pi^* r)$. In addition the product of the former—decreasing—and the latter—increasing—largely cancels out. Thus the pion tensor does not d-scale in R-I. As for R-II, the situation is somewhat more involved. While R_π is still expected to scale proportionally to the in-medium pion mass, the pion mass will not d-scale proportionally to $\sqrt{\langle \bar{q}q \rangle}$ since the bilinear quark condensate tends to zero for $n \gtrsim n_{1/2}$. The chiral symmetry is still spontaneously broken in R-II, hence we expect the GMOR relation, expected to hold in the tree (or mean-field) order medium, to be modified to

$$f_\pi^{*2} m_\pi^{*2} = m_q \langle \bar{q}q \rangle + \sum_{n>1} c_n \langle (\bar{q}q)^n \rangle \qquad (30)$$

$$\Rightarrow \kappa^2 f_{0\pi}^2 m_\pi^{*2} = \sum_{n>1} c_n \langle (\bar{q}q)^n \rangle. \qquad (31)$$

We have indicated by the multiquark (or higher dimension field) condensates a possible nonvanishing contribution to the GMOR mass formula in which the quark condensate $\langle \bar{q}q \rangle$ is vanishing. There are several proposals for specific form for the order parameter(s) [30]. Whatever the precise form may be, multiquark condensates are expected to be quite suppressed in R-II as shown in Ref. [6]. This implies that the pion mass must decrease rapidly in R-II. Despite the rapid decrease of the pion mass in R-II, the pion tensor remains non-d-scaling. This is shown in Fig. 12.

Now we turn to the d-scaling of the ρ-tensor force. At the mean-field (or tree) order in sHLS, the ρ-meson mass will satisfy the KSRF formula with IDD parameters

$$m_\rho^* = \sqrt{a_\rho^* g_\rho^* f_\pi^*}. \qquad (32)$$

In the matter-free vacuum, the KSRF is a low-energy theorem proven to hold to all loop orders in HLS [3,31]. Whether it also holds in medium to all loop-orders or not has not been proven. It seems however reasonable to assume that for a given density, this does hold with g_ρ^* replaced by the effective ρNN coupling constant $g_{\rho NN}$. It has been shown in Ref. [32] that

$$g_{\rho NN}^* = F_\rho^* g_\rho^* \qquad (33)$$

with F_ρ^* that goes to zero at the dilaton-limit fixed point (DLFP), possibly identical to the IR fixed point of [2], independently of how g_ρ^* d-scales. In our application in Sec. V, the effect of F_ρ^* could in principle be included. Therefore we shall leave it out in what follows in our discussion, setting $F_\rho^* = 1$, with the possibility in mind that F_ρ^* effect could further speed up the dropping in R_ρ given below.

While based on the d-scaling argument in Ref. [1] and relying on phenomenological observations [9,18], possible IDD$_{\text{matter}}$ effect in g_ρ^* was ignored in R-I, the IDD$_{\text{matter}}$, as argued in Sec. IV A 2, cannot be ignored in R-II. Noting that

$$m_\rho^*/m_\rho \approx \left(\frac{g_\rho^*}{g_\rho} \right) \left(\frac{f_\pi^*}{f_\pi} \right) \qquad (34)$$

$$\approx \begin{cases} \Phi_I & \text{for R-I} \\ \Phi_{II}^\rho \times \kappa & \text{for R-II} \end{cases}, \qquad (35)$$
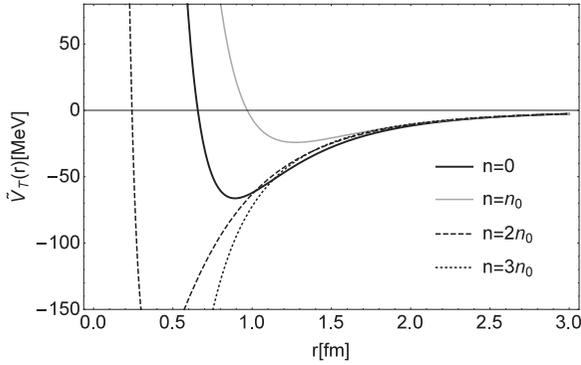
FIG. 1. $\tilde{V}_T(r) \equiv V_T(r)(\tau_1 \tau_2 S_{12})^{-1}$. For illustration, we take $n_{1/2} = 2n_0, \Phi_I = \Phi_{II}^\rho = 1 - 0.15\frac{n}{n_0}$ and $\kappa = 1$.

we find the d-scaling of R_ρ to be of the form

$$R_\rho \approx \frac{g_{\rho NN}^*}{g_{\rho NN}} \frac{m_N}{m_N^*} \frac{m_\rho^*}{m_\rho} \quad (36)$$

$$\approx \left(\frac{g_\rho^*}{g_\rho}\right)^2 \quad (37)$$

$$\approx \begin{cases} 1 & \text{for R-I} \\ \left(\Phi_{II}^\rho\right)^2 & \text{for R-II} \end{cases}. \quad (38)$$

What is crucially important for the structure of the ρ tensor force is the factor R_ρ which changes discontinuously from R-I to R-II across $n_{1/2}$ with the topology change. In R-I, experimentally controlled nuclear processes indicate how Φ_I d-scales. It is a slow decrease reaching $\lesssim 0.8$ at $n \sim n_0$. On the other hand, Φ_{II}^ρ is totally unknown. It is given neither theoretically nor phenomenologically. The only constraint based on HLS [3] is the vector manifestation fixed point at which Φ_{II}^ρ should approach 0 in the chiral limit. If the vector-manifestation (VM) fixed point is $\sim(6-7)n_0$—which is not too far from the density of the interior of ~ 2 solar-mass stars—then Φ_{II}^ρ should drop more rapidly in R-II than in R-I. This point was already emphasized in Ref. [9]. One can see from (38) that there will be a rapid suppression of the ρ tensor force at $n_{1/2}$. This feature is shown in Fig. 1. Just for illustration, we have taken $\Phi_I = \Phi_{II}^\rho = 1 - 0.15\frac{n}{n_0}$ and $\kappa = 1$. In the application to the EoS for nuclear matter and compact-star matter, more realistic d-scaling of the parameters involved will be used.

It is now easy to see how the cusp structure in the S factor at $n_{1/2}$ arises. In the density regime in the vicinity of nuclear matter, the symmetry energy factor S, dominated by the tensor forces, can be reliably approximated by the closure formula [33],

$$S \approx \frac{12}{\bar{E}} \langle \bar{V}_T^2 \rangle, \quad (39)$$

where $\bar{E} \approx 200$ MeV is the average energy typical of the tensor force excitation and $\bar{V}_T$ is the radial part of the net tensor force defined in Fig. 1. The tensor force strength decreasing as density approaches $n_{1/2}$ from below and increasing after above $n_{1/2}$ reproduces the cusp structure [34]. We suggest that

this feature provides, albeit indirect, support to the scaling properties formulated in a general term in Ref. [1].

In Sec. VI, the tensor force structure obtained above, together with the d-scaling properties in Regions I and II, will be confronted with the EoS of nuclear matter and neutron-star matter. For this, the renormalization group implemented $V_{\text{low }k}$ technique will be employed. This will be briefly reviewed in Sec. V.

V. RENORMALIZATION GROUP WITH $V_{\text{low }k}$

As stated in Introduction, the scale-invariant HLS Lagrangian with baryons (bsHLS) can be applied to many-nucleon systems in either RMF involving single decimation or more microscopically with double decimations involving $V_{\text{low }k}$. Here we briefly review the latter approach that will be used in Sec. VI. Details are found in the review articles referred to in this paper. We will essentially follow the strategy used in Ref. [10].

One (in principle) starts with the NN potential V_{NN} gotten from the bsHLS Lagrangian (6) and (22) with the proper IDDs. One then arrives at $V_{\text{low }k}$ *à la* renormalization group technique [7,8]. This consists of decimating the high momentum components from the matching scale or Λ_{eff} to a model-space momentum scale Λ which is not far from the Fermi momentum k_F. In terms of the T matrix, this amounts to computing $V_{\text{low }k}$ as

$$T(k',k,k^2) = V_{NN}(k',k) \\ + \frac{2}{\pi}\mathcal{P}\int_0^\infty \frac{V_{NN}(k',q)T(q,k,k^2)}{k^2 - q^2}q^2 dq, \quad (40)$$

$$T_{\text{low }k}(k',k,k^2) = V_{\text{low }k}(k',k) + \frac{2}{\pi}\mathcal{P} \\ \times \int_0^\Lambda \frac{V_{\text{low }k}(k',q)T_{\text{low }k}(q,k,k^2)}{k^2 - q^2}q^2 dq, \quad (41)$$

$$T(k',k,k^2) = T_{\text{low }k}(k',k,k^2); \quad (k',k) \leqslant \Lambda. \quad (42)$$

Here $\mathcal{P}$ denotes principal-value integration and the intermediate state momentum q is integrated from 0 to ∞ for the whole-space T and from 0 to Λ for $T_{\text{low }k}$.

With the given "bare" effective Lagrangian, if one wishes, one can do a sophisticated effective field theory calculation (such as chiral perturbation theory) to obtain V_{NN}. This should be feasible starting with the effective Lagrangian we are dealing with, i.e., bsHLS. For the exploratory work we are doing here, however, a rigorous EFT calculation is unnecessary. In the present work, as in Ref. [10], we choose the V_{NN} to be the realistic BonnS [35] NN interaction with the IDD dependence encoded in the "bare" parameters taken into account. We shall adopt the vacuum (free-space) parameters chosen in Ref. [35] without adjustments. This is a phenomenologically powerful approach, fit to experimental data in free space as well as in medium to the momentum/energy scale defined by the cutoff Λ. Because we shall calculate the EoS, in particular, the nuclear symmetry energy, $E_{\text{sym}}(n)$ up to $n \sim 5n_0$, we shall use $\Lambda = 3$ fm^{-1} [36]. The $V_{\text{low }k}$ so obtained preserves the low-energy phase shifts in the vacuum (up to energy Λ^2) and the deuteron binding energy of V_{NN}. (For example, the
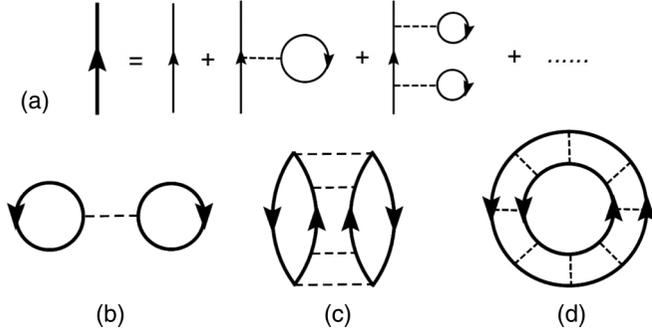
FIG. 2. Diagrams included in the *pphh* ring-diagram summation for the ground-state energy of nuclear matter. Included are self-energy insertions on the single-particle propagator as indicated by (a), and *pphh* ring diagrams by (b)–(d).

deuteron binding energy given by $V_{\text{low } k}$ of $\Lambda = 2.0$ and 3.0 fm^{-1} are both -2.226 MeV.) By construction, $V_{\text{low } k}$ is a smooth "tamed" potential which is suitable for being used directly in many-body calculations.

The first step in the procedure is to verify if in R-I the above $V_{\text{low } k}$ interaction can satisfactorily reproduce the empirical nuclear matter saturation properties (saturation density $n_0 \simeq 0.16$ fm^{-3} and average energy per nucleon $E_0/A \simeq -16$ MeV at saturation). To do this, we shall calculate n_0 and E_0/A using a low-momentum ring-diagram approach [36–40], where the *pphh* ring diagrams are summed to all orders within a model space of the cutoff Λ.

We now briefly describe the above ring-diagram method. The ground-state energy shift is defined as $\Delta E_0 = E_0 - E_0^{\text{free}}$ where E_0 is the true ground-state energy and the corresponding quantity for the noninteracting system E_0^{free}. In the present work, we consider ΔE_0 as given by the all-order sum of the *pphh* ring diagrams as shown in Figs. 2(b)–2(d), they being respectively such a (first-, fourth-, and eighth-order) sring diagram.

In our ring-diagram calculations, we also include Hartree-Fock (HF), single-particle insertions to all orders as illustrated by panel (a) of the figure. Note that each vertex of the diagrams is a $V_{\text{low } k}$ interaction obtained from a density-scaled V_{NN} potential. We include in general three types of ring diagrams, the proton-proton, neutron-neutron, and proton-neutron ones. The proton and neutron Fermi momenta are, respectively, $k_{Fp} = (3\pi^2 n_p)^{1/3}$ and $k_{Fn} = (3\pi^2 n_n)^{1/3}$, where n_p and n_n denote respectively the proton- and neutron-density. The asymmetric parameter is $\alpha \equiv (n_n - n_p)/(n_n + n_p)$. With such ring diagrams summed to all orders, we have

$$\Delta E(n, \alpha) = \int_0^1 d\lambda \sum_m \sum_{ijkl < \Lambda} Y_m(ij, \lambda)$$
$$\times Y_m^*(kl, \lambda) \langle ij | V_{\text{low } k} | kl \rangle, \quad (43)$$

where the transition amplitudes Y are obtained from a *pphh* RPA equation [37,38]. Note that λ is a strength parameter, integrated from 0 to 1. The above ring-diagram method reduces to the usual HF method if only the first-order ring diagram is included. In this case, the above energy shift

becomes $\Delta E(n, \alpha)_{HF} = \frac{1}{2} \sum n_i n_j \langle ij | V_{\text{low } k} | ij \rangle$ where $n_k = (1, 0)$ if $k(\leqslant, >)k_{Fp}$ for proton and $n_k = (1, 0)$ if $k(\leqslant, >)k_{Fn}$ for neutron.

The above $V_{\text{low } k}$ ring-diagram framework has been applied to symmetric and asymmetric nuclear matter [37,38] and to the nuclear symmetry energy [36]. This framework has also been tested by applying it to dilute cold neutron matter in the limit that the $^1S_0$ scattering length of the underlying interaction approaches infinity [39,40]. This limit—which is a conformal fixed point—is usually referred to as the unitary limit, and the corresponding potentials are the unitarity potentials. For many-body systems at this limit, the ratio $\xi \equiv E_0/E_0^{\text{free}}$ is expected to be a universal constant of value $\sim$0.44. (E_0 and E_0^{free} have been defined earlier). The above ring-diagram method has been used to calculate neutron matter using several very different unitarity potentials (a unitarity CD-Bonn potential obtained by tuning its meson parameters, and several square-well unitarity potentials) [39,40]. The ξ ratios given by our calculations for all these different unitarity potentials are all close to 0.44, in good agreement with the quantum Monte Carlo results (see [40] and references quoted therein). In fact our ring-diagram results for ξ are significantly better than those given by HF and BHF (Brueckner HF) [39,40]. It is desirable that the above unitary calculations have provided satisfactory results, supporting the reliability of our $V_{\text{low } k}$ ring-diagram framework for calculating the nuclear matter EoSs.

One should recognize that the above many-body approach is essentially equivalent to doing Landau Fermi-liquid fixed point theory with quasiparticle correlations on top of the Fermi sea treated with $V_{\text{low } k}$ with IDDs implemented, as discussed in Ref. [11]. This procedure is a microscopic improvement on the relativistic mean-field treatment involving single decimation of *bs*HLS Lagrangian. In the application to denser regime going into R-II, the above procedure will be simply extrapolated. It is most likely a valid procedure if the Fermi-liquid structure holds in R-II.

VI. EOS FOR NUCLEAR MATTER AND COMPACT-STAR MATTER

In this section, we shall extrapolate the treatment presented above, verified up to density n_0 and taken to be valid up to $n_{1/2} \sim 2n_0$, to $n > n_{1/2}$ appropriate to massive compact stars. To calculate the EoS for nuclear matter, we use the Bonn *A* potential [29] consistent with the "intrinsic density-dependent" *bs*HLS Lagrangian at the leading order of scale-chiral counting. Here, we should note that we fix the pion exchange potential not to scale in density for both R-I and R-II as we argued on the basis of the pion being a nearly massless Nambu-Goldstone boson. This is a reasonable assumption for a qualitative account for the scaling of the parameters involved. As shown in Ref. [29], the central, spin-spin, and spin-orbit nuclear forces from one-pion exchange are weak or negligible compared with the nuclear forces from the other particles while the tensor force from one-pion exchange is strong. But, as we find in Appendix A, the pion tensor is almost independent of a density.

We start with the "bare" parameters that figure in both R-I and R-II. They are summarized in Table I. As stated, there
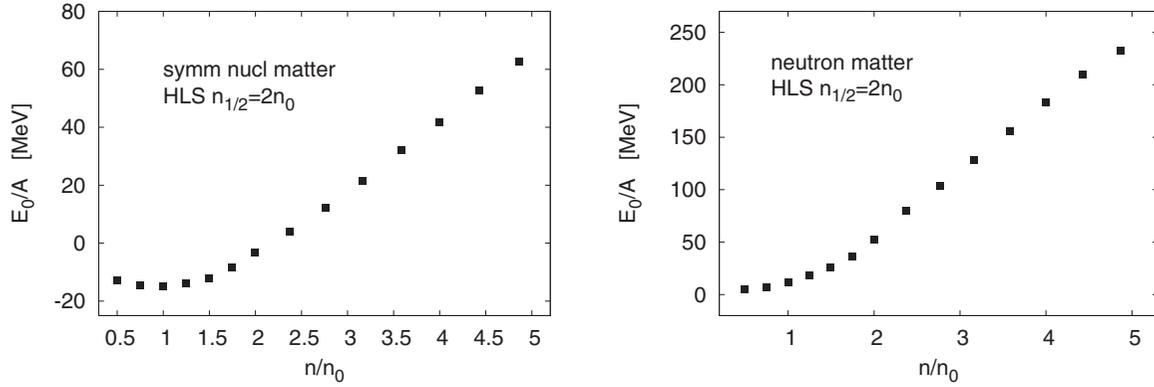
FIG. 3. Ground-state energy E_0 per nucleon of symmetric nuclear matter (left panel) and neutron matter (right panel).

is only one constant, c_I, to be determined in R-I and two constants, κ and c_{II} in R-II. For the numerical work, we will adopt[6]

$$c_I \approx 0.13\text{–}0.20, \quad c_{II} \approx 0.15, \quad \kappa \approx 0.7\text{–}0.8. \quad (44)$$

Before we confront Nature, we discuss how the formalism anchored solely—with no fine-tuning—on the three parameters of (44), fares. We focus on the region R-I where there is only one parameter c_I in the adopted parametrization $\Phi_I = 1/(1 + c_I\, n/n_0)$. In this region near n_0 fairly well-established experimental data are available.

First we recall that in R-I, the scaling is governed entirely by the d-scaling of $f_\sigma^* = \langle\chi\rangle^*$, i.e., the IDD$_{\text{pNG}}$. Although the explicit forms of the masses involved are not known in terms of the condensates, $\langle\bar{q}q\rangle$ and $\langle G^2\rangle$, we learn from CT theory [2] that the masses of nucleon and dilaton are dominated by $\langle G^2\rangle$ whereas the masses of the vector mesons are more crucially controlled by $\langle\bar{q}q\rangle$ in particular in R-II. This means that as the condensate $\langle\bar{q}q\rangle$ gets averaged to zero at $n_{1/2}$ with the possible multiquark condensates nonzero but suppressed, the vector-meson masses will be more strongly affected by density than the masses of nucleon and dilaton. Thus one expects that c_I's for ρ and ω are larger than c_I's for σ and nucleon. Now suppose we simply ignore this feature and take one universal c_I. The result is given in Appendix B. One sees unambiguously that neither the equilibrium density nor the binding energy can be gotten with only the c_I parameter. As we will see below, however, only a small adjustment within the given range of c_I's, with the above scale symmetry feature taken into account, can reproduce fairly well the nuclear-matter observables. This exercise demonstrates that Nature seems to be *unreasonably* fine-tuned.

Given that a universal c_I fails quite dramatically to reproduce Nature, we make, eschewing an extreme fine-tuning,

minimal adjustments for different mesons, within the range given in Eq. (44), to calculate the ground-state energies of nuclear matter using the ring-diagram method with the density scaled $V_{\text{low}\,k}$ interaction as described earlier. The small differences in c_I may be considered as $1/N_c$ corrections in different channels in the "bare" parameters of the in-medium Lagrangian.

Our results for symmetric nuclear matter and neutron matter are shown respectively in the left and right panels of Fig. 3. The scaling parameters employed are shown in Table II.

For R-I, as indicated in Fig. 3, we determine c_I's to provide a satisfactory description of the saturation properties of symmetric nuclear matter, giving saturation energy $E_0/A = -15.1$ MeV, the saturation density $n_{\text{sat}} = 0.16$ fm^{-3} and the compression modulus $K = 183.2$ MeV. The compression modulus comes out somewhat smaller than the value often quoted, $\gtrsim 200$ MeV. This approach predicts a softer EoS for nuclear matter than for neutron matter (given below). We will return to this matter later. Table II shows that the scaling in R-I is consistent with the expectation that c_I's for ρ and ω should be lager than c_I's for σ and nucleon. It is to be noted that the inequality $c_I^{N,\sigma} < c_I^{\rho,\omega}$ argued for in the context of chiral-scale symmetry is crucial for the fit to Nature. Thus Nature seems to exercise a fine-tuning that goes beyond

_____

[6]The constant c_I that figures in the double decimation $V_{\text{low}\,k}$ approach needs not be the same as the single-decimation value found in the calculation of the anomalous orbital gyromagnetic ratio δg_l measured in Pb [41]. In fact, it is found to be $c_I \approx 0.28$, somewhat larger than the range given in Ref. (44). There is no discrepancy here. The latter subsumes some part of quasiparticle interactions captured in the Landau fixed-point parameters F_1 and F_2.

TABLE I. The d-scaling "bare" parameters of bsHLS Lagrangian (6) in R-I and (22) in R-II. Φ_{II}^ω is unknown if U(2) symmetry is broken down as described in Appendix C. How it is deduced is discussed in the text.

R-I	$\dfrac{m_N^*}{m_N} \approx \dfrac{m_\sigma^*}{m_\sigma} \approx \dfrac{m_V^*}{m_V} \approx \dfrac{f_\sigma^*}{f_{0\sigma}} \approx \dfrac{f_\pi^*}{f_{0\pi}} \approx \Phi_I$
	$\dfrac{g_\sigma^*}{g_\sigma} \approx \dfrac{g_V^*}{g_V} \approx 1$
	$\dfrac{g_{\pi NN}^*}{g_{\pi NN}} \approx \dfrac{g_A^*}{g_A} \approx \Phi_I \quad \& \quad \dfrac{m_\pi^*}{m_\pi} \approx (\Phi_I)^{\frac{1}{2}}$
	$\Phi_I = \dfrac{1}{1 + c_I \frac{n}{n_0}}$
R-II	$\dfrac{m_N^*}{m_N} \approx \dfrac{m_\sigma^*}{m_\sigma} \approx \dfrac{f_\sigma^*}{f_{0\sigma}} \approx \dfrac{f_\pi^*}{f_{0\pi}} \approx \kappa$
	$\dfrac{g_\sigma^*}{g_\sigma} \approx 1 \quad \& \quad \dfrac{g_V^*}{g_V} \approx \Phi_{II}^V$
	$\dfrac{g_{\pi NN}^*}{g_{\pi NN}} \approx \dfrac{g_A^*}{g_A} \approx \kappa \quad \& \quad m_\pi^{*2} \approx \dfrac{1}{f_{0\pi}^2 \kappa^2} \sum c_n \langle(\bar{q}q)^n\rangle$
	$\dfrac{m_\rho^*}{m_\rho} \approx \dfrac{g_\rho^*}{g_\rho} \quad \& \quad \dfrac{m_\omega^*}{m_\omega} \approx \kappa \sqrt{\dfrac{a_\omega^*}{a_\omega} \dfrac{g_\omega^*}{g_\omega}}$
	$\Phi_{II}^\rho = 1 - c_{II}\dfrac{n}{n_0} \quad \& \quad \Phi_{II}^\omega = \,??$

TABLE II. The precise values for the scaling parameters in R-I and R-II. The scaling properties shown above are consistent with the scaling of the parameters in Table I. As stated in the text, the pionic parameters are taken not to scale in both R-I and R-II.

	R-I	R-II
$\frac{m_N^*}{m_N}$	$\frac{1}{1+0.12\frac{n}{n_0}}$	0.71
$\frac{m_\sigma^*}{m_\sigma}$	$\frac{1}{1+0.12\frac{n}{n_0}}$	0.75
$\frac{m_\rho^*}{m_\rho}$	$\frac{1}{1+0.14\frac{n}{n_0}}$	$1-0.15*\frac{n}{n_0}$
$\frac{m_\omega^*}{m_\omega}$	$\frac{1}{1+0.14\frac{n}{n_0}}$	$0.73\frac{g_\omega^*}{g_\omega}$
$\frac{g_\rho^*}{g_\rho}$	1	$1-0.15*\frac{n}{n_0}$
$\frac{g_\omega^*}{g_\omega}$	1	$1-0.053*\frac{n-n_{1/2}}{n_0}$

the general framework adopted in our approach for the EoS considered for compact stars. The coupling constants g_ρ^* and g_ω^* associated with IDD$_{\text{matter}}$ do not scale in this region.

The scaling in R-II is our main interest. It will be shown below that the scaling in Table II, qualitatively consistent to that of Table I, produces the EoS for nuclear matter, which is compatible with Nature. For R-II, we take $\Phi_{II}^\rho = 1 - 0.15(n/n_0)$ for the VM behavior of the ρ with $n_c \approx (6$–$7)n_0$ and $m_\rho^*/m_\rho = g_\rho^*/g_\rho = \Phi_{II}^\rho$. The oversimplified parametrization for m_ρ^* and g_ρ^* may be the cause of the most likely artificial gap in the ground-state energy at $n = n_{1/2}$. To remove this gap and get the resulting EoS within the empirical constraint of Danielewicz [42], we adjust the values for κ's of σ, ω and the nucleon. As for the ω properties, we take a scaling drastically different from that of the VM behavior of the ρ, say, $\Phi_{II}^\omega = 1 - 0.053(n - n_{1/2})/n_0$. Given that the attraction is largely controlled by the dilaton exchange whose mass remains unscaling or at most slowly scaling, the repulsion due to the ω exchange is highly constrained, so that a faster decrease of the g_ω^*/g_ω cannot be accommodated. Likewise a substantial decrease of a_ω^* would not be allowed if one were not to exceed the Danielewicz constraint. Therefore we have simply taken $a_\omega^* = a_\omega$.

As indicated by Eq. (2), the nuclear symmetry energy $E_{\text{sym}}(n)$ is given by $E_0(n,1)/A - E_0(n,0)/A$. [Here E_{sym} is the same as the S factor of Eq. (2).] In Fig. 4 we present our calculated symmetry energies and compare them with their empirical values. Li *et al.* [43] have suggested an empirical relation

$$E_{\text{sym}}(n) \approx 31.6 \text{ MeV}(n/n_0)^\gamma; \quad \gamma = 0.69\text{–}1.1, \quad (45)$$

for constraining the density dependence of the symmetry energy. The upper ($\gamma = 1.1$) and lower ($\gamma = 0.69$) constraints are also plotted in the figure, labeled as A and B respectively. Tsang *et al.* [44] proposed an empirical formula for the symmetry energy, namely

$$E_{\text{sym}}(n) = \frac{C_{s,k}}{2}\left(\frac{n}{n_0}\right)^{2/3} + \frac{C_{s,p}}{2}\left(\frac{n}{n_0}\right)^{\gamma_i}, \quad (46)$$
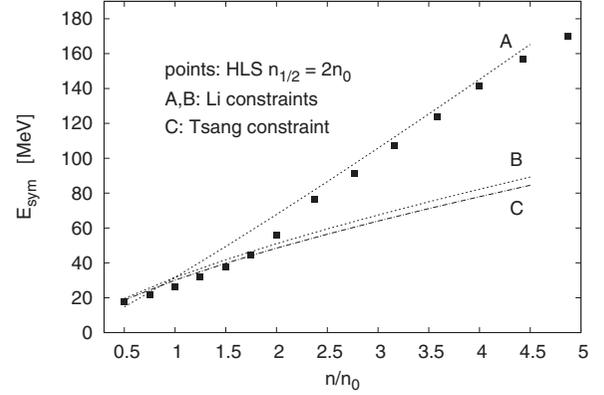
FIG. 4. Comparison of our calculated symmetry energies $E_{\text{sym}}(n)$ with the empirical ones of Li *et al.* [43] and Tsang *et al.* [44]. It is worth noting that the predicted symmetry energy manifests a shift from soft to hard at $n_{1/2}$ reflecting the classical cusp structure in the skyrmion description of the topology change.

where $C_{s,k} = 25$ MeV, $C_{s,p} = 35.2$ MeV, and $\gamma_i \approx 0.7$. This formula is also plotted in Fig. 4, labeled as C. As seen, our calculated E_{sym} is slightly lower than the constraints in the low-density region, and is close to Li's upper constraint in the high-density region. It is noteworthy that the S is relatively soft at low densities and hard at high densities, the changeover occurring at the crossover density $n_{1/2}$. This is a prediction of our theory.

Extensive studies have been carried out by Lattimer and Lim [45] concerning the empirical constraints on E_{sym} and L [defined as $3u(dE_{\text{sym}}/du), u \equiv n/n_0$] at density $n = n_0$. Their results deduced from a wide range of observables including nuclear masses, nuclear giant dipole resonances, astrophysics, and neutron skins of the *Sn* isotopes suggested $28 \lesssim E_{\text{sym}}/\text{MeV} \lesssim 32$ and $40 \lesssim L/\text{MeV} \lesssim 60$. Our results for them are given in Table III, indicated by "*bs*HLS." Our E_{sym} is ~ 27 MeV which is slightly smaller than the empirical value of ~ 30 MeV. Our L value of ~ 57 MeV is in satisfactory agreement with the empirical values of Lattimer, but slightly lower than Li's lower and Tsang's constraints. (The two entries in row 2 of the Table III are respectively the L values given by Li's lower and upper constraints.)

It is of interest and useful to calculate the pressure-density EoS $p(n)$ and compare it with the empirical constraints of Danielewicz *et al.* [42]. This EoS is given by using

$$\frac{E_0}{A} = a\left(\frac{n}{n_0}\right) + b\left(\frac{n}{n_0}\right)^c \quad (47)$$

TABLE III. Comparison of our calculated E_{sym} and L (*bs*HLS) at $n = n_0$ with the empirical values of Li *et al.* [43], Tsang *et al.* [44], and Lattimer *et al.* [45].

$E_{\text{sym}}/\text{MeV}$	L/MeV	
27	57.3	*bs*HLS
31.6	65.4–104.2	Li
30.1	62.0	Tsang
28–32	40–60	Lattimer
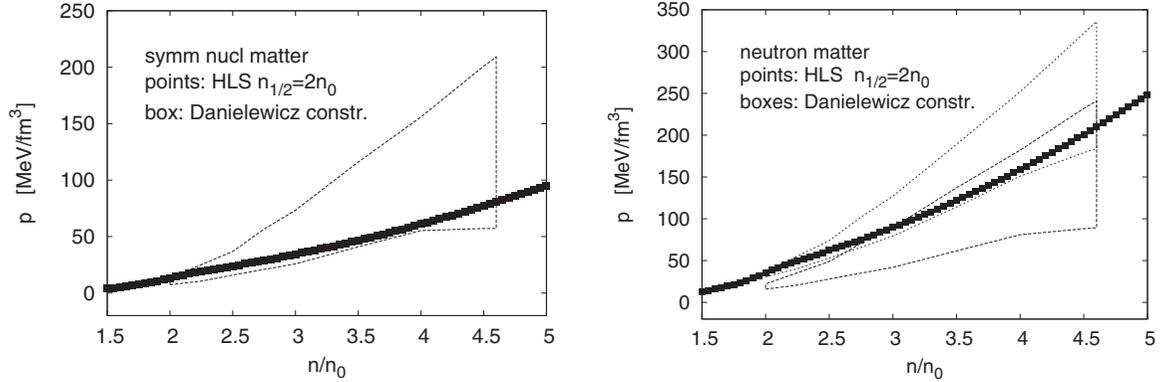
FIG. 5. Calculated pressure in symmetric nuclear matter (left panel) and the same in neutron matter (right panel) compared with the Danielewicz constraints [42].

to fit E_0/A in Fig. 3, where

$$p(n) = n \frac{d\epsilon(n)}{dn} - \epsilon(n) \tag{48}$$

and the energy density is

$$\epsilon(n) = n \left[\frac{E_0(n)}{A} + m_N \right] \tag{49}$$

with m_N being the nucleon rest mass. Our result for $p(n)$ of symmetric nuclear matter is shown in the left panel of Fig. 5. Our EoS is generally in agreement with the Danielewicz constraint although being rather close to the lower boundary of the constraint box.

Our calculated $p(n)$ for neutron matter is shown in right panel of Fig. 5, and as shown it is generally in agreement with the Danielewicz constraints. There are two Danielewicz constraints in this case, one for the empirical stiff EoS (upper box) and the other for the soft one (lower box). Our $p(n)$, being near the lower boundary of the upper (stiff) box, is mostly in the overlapping region allowed by both constraints.

Our neutron-matter EoS may be considered as "medium stiff." Can it support a massive neutron star such as the $2M_\odot$ one recently observed by Antoniadis *et al.* [46]? From the neutron matter EoS we can calculate the properties of pure neutron stars. This is of much interest, and could provide a useful test of our neutron matter EoS in the high density region. We have done so and our results are presented below. We first calculate the pressure-energy EoS $p(\epsilon)$ and then various neutron-star properties are obtained from solving the Tolman-Volkov-Oppenheimer (TOV) equations with the above EoS as the input (see, e.g., [38]).

In Fig. 6 our calculated neutron-star mass-radius relation is shown. Our maximum-mass neutron star has mass $M \simeq 2.07M_\odot$, and radius $R \simeq 11.7$ km. With the weak equilibrium, not included here, taken into account, we expect that the maximum mass will come down a bit. This calculated mass is close to the mass $2.01 \pm 0.04M_\odot$ of the recently observed relativistic pulsar [46]. It may be worth mentioning that the central density of our maximum-mass neutron star is merely $\sim 5.6n_0$ as indicated in Fig. 7. At this density, we have found that our EoS is within the causal limit; for example our EoS

has $v_{sound}/c \sim 0.65$ at densities between $n/n_0 = 5.0$ and 6.0. This is shown in Fig. 8. What is significant in this result is that the change in the d-scaling in the parameters of the effective Lagrangian in R-II stabilize the sound velocity within the causal limit. Without the topology change, the causality would be violated at the density reached in massive stars.

Lattimer and Schutz have proposed an empirical relation

$$I \simeq (0.237 \pm 0.008)MR^2$$

$$\times \left[1 + 4.2 \frac{M}{M_\odot} \frac{km}{R} + 90 \left(\frac{M}{M_\odot} \frac{km}{R} \right)^4 \right] \tag{50}$$

constraining M, R and the moment of inertia I of neutron stars [47]. In solving the TOV equations, we integrate outward from the center of the neutron star till its edge where pressure is zero. In this process we know the matter distribution at all radii and thus can calculate its moment of inertia I. In Fig. 9, we compare this I (A) with the one given by the above relation using our calculated M and R as inputs (B). This comparison provides a check of our calculated density profile of the neutron star. As seen, our results are in good agreement with the empirical values for neutron stars with mass less than
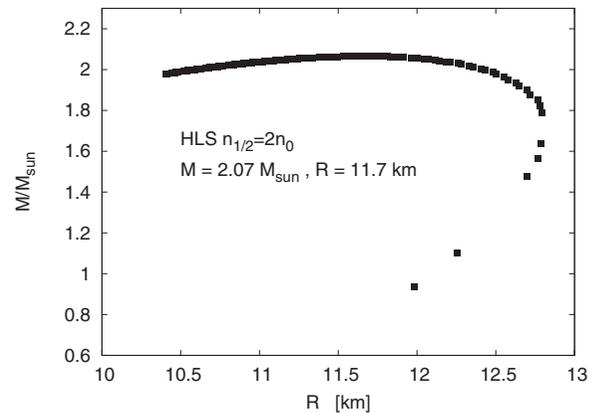
FIG. 6. Mass-radius relation of pure neutron stars calculated from the EoS of Fig. 5 (right panel). Our EoS does not contain the part of EoS of low densities appropriate for the surface region and hence cannot account for the low-mass stars.
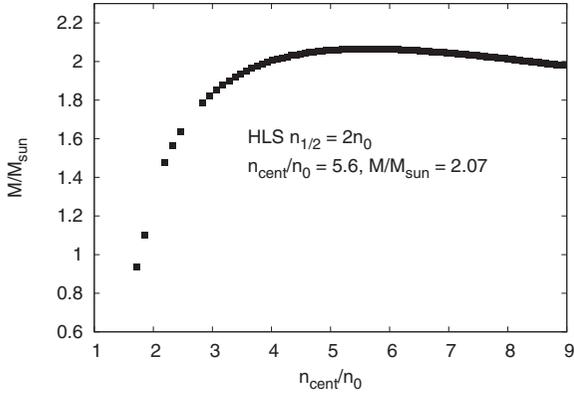
FIG. 7. Central densities of pure neutron stars of Fig. 6.

FIG. 9. Moment of inertia of neutron stars of Fig. 6.

$\sim 1.4 M_\odot$ But at larger masses, there is significant difference between the two. As of now, we are not sure about the reason for this difference. In our present calculation, neutron stars are assumed to be composed of pure neutron matter. Maybe the above difference is related to this assumption; namely this assumption is possibly adequate for light neutron stars but not so for heavier ones. For neutron stars of mass larger than $\sim 1.4 M_\odot$, the presence of other constituents such as protons [38] and/or strange particles may be necessary. In the following section, we consider the latter possibility.

VII. STRANGENESS PROBLEMS

We discuss in this section how the approach formulated in flavor SU(2) exploited above for the EoS of compact stars can be applied to strangeness in compact-star matter, namely, the hyperon puzzle and kaon condensation problem. In the treatment given above, the effect of the dilaton which has a natural habitat in flavor SU(3) is projected into the SU(2) HLS Lagrangian. To be fully realistic in addressing strangeness, one should resort to a three-flavor scale-invariant HLS Lagrangian

FIG. 8. The sound velocity obtained from a fitting formula that reproduces the EoS of the neutron matter in Fig. 3. Near the crossover density $n_{1/2} = 2n_0$, there is some discontinuity—most likely artificial—in velocity caused by the sharp demarcation of the parameter scaling, which turns out to be sensitive to the way the fitting is done.

with the dilaton treated on the same footing with kaons [2]. To address the EoS of compact stars with strangeness duly taken into account, the $V_{\mathrm{low}\,k}$ RG approach would then have to be extended to three flavors. Unfortunately such a three-flavor $V_{\mathrm{low}\,k}$ formulation is not yet available. In this section, we sketch how to address some of the issues involved with strangeness in the two-flavor framework developed applied in Sec. VI.

A. Hyperon problem

In developing the EoS in Sec. VI, strangeness degrees of freedom have been ignored. It is known that if the strangeness enters in compact-star systems, then the EoS can become too soft and massive stars of ~ 2 solar mass cannot be supported. For instance, this applies to the presence of hyperons. Simple energetic considerations suggest that hyperons should be present at high density in compact-star matter [48]. The lowest-lying hyperon Λ, with its attractive interaction, is estimated to appear at matter density $\sim 2n_0$ with the others possibly appearing at higher density. What this suggests is that the hyperons could appear at about the same density as the one at which the half-skyrmion phase appears in the skyrmion matter. If this were the case, then the prediction made in Section VI would make no sense without the hyperonic degree of freedom taken into account.

Since a $V_{\mathrm{low}\,k}$ formalism for 3-flavor is not available, we address this problem using a mean-field approach with the two-flavor bsHLS Lagrangian employed in Section VI. One can think of this approach as a "single-decimation" RG approach as introduced in Ref. [9] in contrast to the double-decimation applied above. This approach was applied with success to the calculation of the anomalous gyromagnetic ratio in heavy nuclei δg_l [41].

We find that with the scaling property of the "bare" parameters of the Lagrangian obtained above, the interactions between Λs and nucleons become sufficiently repulsive at a density $n \lesssim 3n_0$ so as to prevent the Λs from appearing in the system. Our reasoning relies on what we shall refer to as "Bedaque-Steiner" constraint

In a highly sophisticated phenomenological study using a Monte Carlo simulation over parameters that enter in the EoS for symmetric and asymmetric nuclear matter such as the compression modulus K and L, symmetry energies S and S_Λ,

Bedaque and Steiner obtain the range of density Δ constrained by hydrodynamic stability of the system, that ensures that stars with $M > 2M_\odot$ could be supported [49]. The Δ is then the range of density beyond which the in-medium Λ mass becomes greater than the vacuum value. One expects – and it is confirmed experimentally – that the Λ-nucleon interaction is attractive at normal nuclear matter density, so Λs can be bound in nuclear matter. In compact star matter, as density increases, the chemical potential difference between neutron and proton increases and it can become energetically favored to have spontaneous creating of hyperons in the system. It turns out that this can happen when density reaches roughly twice the normal nuclear matter density unless the attractive interaction is canceled by repulsive mechanisms. The instability generated by the presence of hyperons at that low density is the hyperon problem. The Δ then stands for the range of density at which the Λ-interactions must be repulsive enough to make the in-medium Λ mass be greater than the vacuum mass. The analysis by Bedaque and Steiner establishes that the range of Δ required is $1 \lesssim \Delta/n_0 \lesssim 3$.

It is feasible, with some reasonable assumptions, to calculate the effective mass of Λ in medium using the *bs* HLS formalism applied above. We do this using an RMF approximation with the Lagrangian (6) and (22).

In the mean field approximation, the chemical potential for the Λ in medium gets contributions from two sources, one from the IDD$_{\mathrm{pNG}}$ in the "bare" mass parameter $m_\Lambda^* \approx \frac{f_\sigma^*}{f_{0\sigma}} m_\Lambda$ and the other from the potential terms coming from Λ-nuclear coupling via σ and ω exchanges as depicted in Fig. 10,

$$\mu_\Lambda = m_\Lambda^* - \frac{g_{\sigma\Lambda}^* g_{\sigma N}^*}{m_\sigma^{*2}} n_s + \frac{g_{\omega\Lambda}^* g_{\omega N}^*}{m_\omega^{*2}} n, \qquad (51)$$

where n_s and n are, respectively, nucleon scalar density and nucleon number density as defined in Fig. 10. The notations for (σ, ω) coupling to Λ and N are self-evident. The asterisk stands for d-scaling parameters.

Apart from the Λ coupling to the mesons, the large cancellation between the σ attraction and the ω repulsion responsible for small binding energy for nuclear matter must take place also in this case. In fact, using the standard
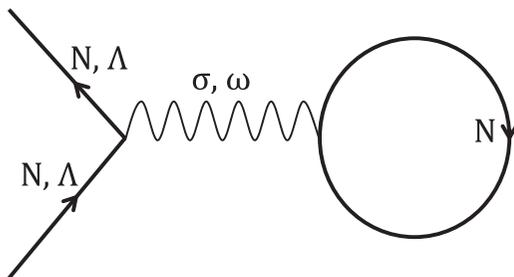
FIG. 10. Tadpole diagram for self-energies for the nucleon N and the hyperon Λ in medium. The loop corresponds to the nucleon scalar density $n_s = \langle \bar{N} N \rangle$ for coupling to σ and the nucleon number density $n = \langle N^\dagger N \rangle$ for coupling to ω.

TABLE IV. The "bare" parameter scaling for mean-field estimate of Λ mass shift in dense matter. The only scaling parameter is chosen to be $c_I = 0.13$ as in Sec. VI. The vacuum scalar (dilaton) mass is taken to be $m_\sigma = 720$ MeV so as to give $\sim$600 MeV at nuclear matter density appropriate for RMF approach. We have taken $\frac{3}{2} g_{\omega\Lambda} = g_{\omega N} = 12.5$ and $\frac{3}{2} g_{\sigma\Lambda} = g_{\sigma N} = m_N/f_\pi$. The empirical values $m_N = 939$ MeV, $m_\Lambda = 1116$ MeV, and $m_\omega = 783$ MeV are taken from the particle data booklet. The scaling $\frac{g_\omega^*}{g_\omega} \approx 1 - 0.053 \frac{n - n_{/2}}{n_0}$ is taken as the "best fit" from the analysis in Sec. VI.

	Parameters for Λ mass shift
R-I	$\frac{m_\Lambda^*}{m_\Lambda} = \frac{m_N^*}{m_N} = \frac{m_\sigma^*}{m_\sigma} = \frac{m_\omega^*}{m_\omega} = \frac{1}{1 + c_I * \frac{n}{n_0}}$
	$\frac{g_{\omega\Lambda}^*}{g_{\omega\Lambda}} = \frac{g_{\omega N}^*}{g_{\omega N}} = \frac{g_\omega^*}{g_\omega} = \frac{g_{\sigma\Lambda}^*}{g_{\sigma\Lambda}} = \frac{g_{\sigma N}^*}{g_{\sigma N}} = 1$
R-II	$\frac{m_\Lambda^*}{m_\Lambda} = \frac{m_N^*}{m_N} = \frac{m_\sigma^*}{m_\sigma} = \kappa = \frac{1}{1 + c_I * \frac{n_{1/2}}{n_0}}$
	$\frac{m_\omega^*}{m_\omega} = \kappa \frac{g_\omega^*}{g_\omega}$ & $\frac{g_{\omega\Lambda}^*}{g_{\omega\Lambda}} = \frac{g_{\omega N}^*}{g_{\omega N}} = \frac{g_\omega^*}{g_\omega}$
	$\frac{g_{\sigma\Lambda}^*}{g_{\sigma\Lambda}} = \frac{g_{\sigma N}^*}{g_{\sigma N}} = 1$

constituent quark counting,[7] we may take $g_{\sigma\Lambda} \approx \frac{2}{3} g_{\sigma N}$ and $g_{\omega\Lambda} \approx \frac{2}{3} g_{\omega N}$, the 2/3 factor accounting for the two nonstrange quarks in Λ vs 3 in nucleon. Then

$$\mu_\Lambda = m_\Lambda^* + \frac{2}{3}\left(-\frac{g_{\sigma N}^{*2}}{m_\sigma^{*2}} n_s + \frac{g_{\omega N}^{*2}}{m_\omega^{*2}} n \right). \qquad (52)$$

This indicates that the Λ effective mass shift $\mu_\Lambda - m_\Lambda$ will become positive near $\sim 2n_0$ as in the symmetric nuclear matter.

To make a rough estimate of the Λ mass shift in dense medium, we take into account the d-scaling of the parameters in the *bs*HLS Lagrangian in the mean-field calculation which corresponds to the "single-decimation procedure" of [9]. In doing this, it is important to recognize the scaling parameter c_I in this procedure could be different, i.e., renormalized, from the IDD coefficient entering into the double-decimation procedure with $V_{\mathrm{low}\,k}$ employed in Sec. VI. The reason is that in the single-decimation procedure of RMF, as noted above, the scaling function Φ_I is related to the Fermi-liquid fixed-point parameters as shown in Ref. [41] and encodes certain nonperturbative quasiparticle interactions on top of the IDD effects manifesting scale-chiral symmetry.

We ignore this subtlety that we expect to be of higher-order fluctuation corrections. Thus we take c_I as used in the $V_{\mathrm{low}\,k}$ calculation, $c_I \approx 0.13$. The scaling and the constants for the dilaton and ω used in the calculation—which are consistent with the property of nuclear matter treated in the mean field of the given Lagrangian—are summarized in Table IV.

The result is plotted in Fig. 11. We see that $\mu_\Lambda - m_\Lambda$ crosses zero at a density $1.5 < n/n_0 < 2.0$. The result is insensitive to the demarcation density for the regions. In fact what comes out in the mean field is quite easy to understand. Since m_Λ^* stops dropping with f_σ^* stabilizing at $2n_0$, what matters is

---

[7]In CT theory, the dilaton is a strong mixture of the quarkonium component and the gluonium component, so this quark counting may not be reliable. However we do not expect it to deviate much from 1.
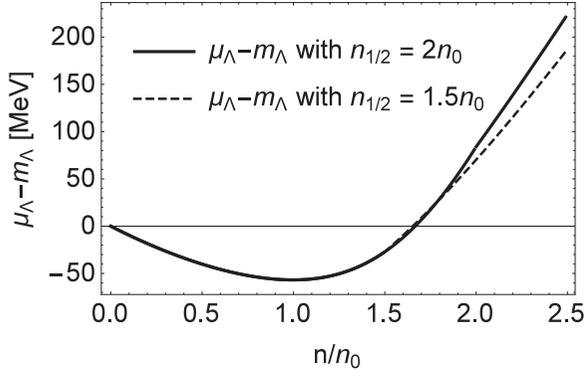
FIG. 11. $\mu_\Lambda - m_\Lambda$ vs n/n_0 calculated with the scaling parameters determined in the theory and summarized in Table IV. The demarcation density was chosen for $n_{1/2} = (1.5, 2.0)n_0$. The density at which the mass shift crosses zero corresponds to Δ of [49].

the interplay of the ratio $\left(\frac{g^*}{m^*}\right)^2$ for the scalar and vector mesons—with an opposite sign—multiplied, respectively, by the scalar density n_s and by the baryon number density n. The vector repulsion wins over the scalar attraction as density increases in the same way as it does in nuclear matter. Although the estimate is admittedly approximate—and it could be done much more realistically in the $V_{\text{low }k}$ approach used above, the BS constraint [49] met by our analysis is most likely robust. We conclude from this that within the formalism developed in Ref. [1] and with the prescription given in Ref. [49], the hyperon problem does not arise in compact stars and hence the EoS discussed in Sec. VI with hyperon degrees of freedom ignored could stay valid.

B. Kaon condensation

In the literature, the hyperon problem is treated independently of kaon condensation. We believe this is incomplete if not incorrect. In fact both hyperons and kaons figure together in flavor SU(3) chiral Lagrangian and should be treated on the same footing. As will be discussed below, to $\mathcal{O}(N_c^0)$, hyperons and condensed kaons are likely to appear at the same density, with the possibility that higher-order corrections in $1/N_c$ could trigger hyperons to appear *before* condensed kaons. In the preceding section, it was suggested that hyperons may be ignored in the EoS. The argument developed there was quite simple. In a close parallel to nuclear matter at high density where the repulsion between nucleons in exchange of ω mesons overpowers the attraction due to scalar exchanges at densities near $2n_0$, Λ-nuclear interactions make the effective mass of a Λ in medium greater than that of a Λ in the matter-free vacuum. In this section, we explore whether a related mechanism could be applied to avoid the "kaon condensation problem."

1. Callan-Klebanov skyrmion

We first address the issue as to whether kaons condense before or after the appearance of hyperons. At present, to the best of our knowledge, the only way this problem can be addressed in a tractable approximation in consistency with the

basic premise of QCD—such as large N_c—is the skyrmion description in which both kaons and hyperons can be treated on the same footing with a same Lagrangian. This matter was first discussed in Ref. [50] employing the successful Callan-Klebanov bound-state model [51]. In this model, antikaons K^- are bound to the SU(2) skyrmion to yield hyperons. A highly nontrivial and surprising observation is that this model interpolates kaons between the chiral limit ($m_K \to 0$) and the Isgur-Wise heavy-quark limit ($m_K \to \infty$). The model can be applied to nuclear matter by putting the CK skyrmions on crystal lattice. It was shown [50] that put on a crystal, the energy difference between the lowest-lying hyperon Λ and the nucleon N in medium comes out

$$E_\Lambda^* - E_N^* = \omega_K^* + \mathcal{O}(N_c^{-1}), \tag{53}$$

where the asterisk represents medium dependence. Note that the in-medium kaon mass is of N_c^0 in the N_c counting. It is fortunate that the leading $\mathcal{O}(N_c)$ term and the flavor singlet $\mathcal{O}(N_c^0)$ Casimir energy term—which is extremely difficult to calculate—cancel out in the difference.

Now, the Λs will appear in the compact star matter when

$$\mu_e \geqslant E_\Lambda^* - E_N^*, \tag{54}$$

where μ_e is the electron chemical potential which is equal to $\mu_n - \mu_p$ in weak equilibrium. On the other hand, kaons will appear by the weak process $e^- \to K^- + \nu_e$ when

$$\mu_e \geqslant m_K^*. \tag{55}$$

Therefore to the leading order in N_c in QCD, hyperons and condensed kaons populate compact stars simultaneously. Which one appears first in the single Lagrangian description depends on $\mathcal{O}(1/N_c)$ hyperfine corrections, namely, when the skyrmion-kaon system is rotationally quantized. A simple quasiparticle approximation leads to

$$E_\Lambda^* - E_N^* = \omega_K^* + \frac{3}{8\Omega^*}(c^{*2} - 1), \tag{56}$$

where $\Omega > 0$ is the moment of inertia of skyrmion rotator and c^* is the in-medium hyperfine coefficient multiplying the effective spin operator of strangeness -1. The coefficient c is highly model dependent even in the matter-free space [51], so it is unknown in dense matter except in the large N_c limit and also in the chiral limit. In either or both of these limits, $c^* \to 1$. In the matter-free space, it is found to be $c^2 \sim 0.5$. Although presently there is no proof, it seems likely that $c^{*2} < 1$ in medium, approaching 1 from below near chiral restoration. If this is the case, that would suggest that hyperons appear before kaons condense[8] and they ultimately join in the vicinity of chiral restoration. It is however difficult to be more precise on this point since the effect is at $\mathcal{O}(N_c^{-1})$ and at that order there are many other corrections of the same order, such as higher-order nuclear correlations, that go beyond the mean-field order as in the $V_{\text{low }k}$ approach of Sec. VI. We are therefore unable to conclude that the absence of hyperons *à la* Bedaque and Steiner precludes kaon condensation.

---

[8]This conclusion is opposite to what was aimed at or conjectured by [50].

2. Relativistic mean field with bsHLS

If hyperons do not figure in the EoS considered in Sec. VI and kaons condense only after hyperons appear as suggested above, does it mean that kaon condensation can also be ignored? In order to address this question, we need a more detailed analysis within the framework developed in the paper. In the absence of $V_{\text{low }k}^{\text{SU(3)}}$ approach, the best we can do is an RMF approach using the bsHLS Lagrangian with kaons implemented as "heavy" mesons with the scaling parameters in the SU(2) sector fixed in Sec. VI. A similar approach is discussed with the dilaton treated differently from ours in Ref. [52].

In RMF, we can follow the argument given in Ref. [25]. In mean field, the kaon in medium receives mass shift by the tadpole in Fig. 10 with the left baryon (N, Λ) replaced by K^-. There is one striking difference between the baryon and the kaon. Unlike in the case of baryon where the scalar contribution is canceled by the vector contribution, for the K^-, both come in with the same sign thanks to the G parity and the attractions add. This immediately precludes the mechanism that prevented the appearance of hyperons for $n \gtrsim 2n_0$ for preventing kaon condensation. This would mean that kaon condensation could intervene at higher densities where hyperons are not present.

What can prevent this was suggested in Ref. [53] where the authors introduce higher-order nuclear correlations that involve repulsions in nucleon-nucleon interactions. The mechanism proposed in Ref. [53] is shown to push n_K to $\gtrsim 6n_0$, above the central density of $\sim$2-solar mass stars. This mechanism is not captured in the mean field with our bsHLS. It could however be captured in a three-flavor microscopic $V_{\text{low }k}$ approach, a project relegated to a future research.

Other considerations

(1) Of interest is the role of the IR fixed point of scale symmetry at which the dilaton mass is to vanish (in the chiral limit) [2]. If the IR fixed point of scale symmetry is near n_{cent}, the possibility we have ignored in this paper, then one would have to consider the possible breakdown of Fermi-liquid structure in the baryonic matter involved as discussed in Ref. [54]. The breakdown of Fermi-liquid structure would make this problem a whole new ballgame. Kaon condensation in non-Fermi liquid is a totally unknown object.

(2) An alternative scenario is that if the kaon condensation threshold density is pushed up by the mechanism for the hyperon solution, then condensed kaons could be in a peaceful coexistence with non-Fermi-liquid baryons in a form similar to strong-coupling strange quark matter co-existing with hadronic matter with no phase transition as discussed in a phenomenological model [55] or three-layer structure consisting of hadrons, condensed kaons, and strange quarks with a kaon-condensed state playing a doorway state to strange quark matter [56].

VIII. CONCLUSION

In this paper, we have constructed an "intrinsic density-dependent" scale-invariant hidden local symmetry ("bsHLS") Lagrangian with baryons included explicitly, capturing

sliding-vacuum properties induced by densities, and applied it to nuclear matter and compact-star matter. In determining the "bare" parameters of the bsHLS Lagrangian, we exploited the structure of baryonic matter present in the skyrmion description, namely, the skyrmion–half-skyrmion topology change at a density above that of the normal nuclear matter, and determined the IDD parameters in two regions of density R-I and R-II with the demarcation at the topology change density $n_{1/2} \approx 2n_0$. It turns out, remarkably, that the scaling of the parameters of the bare Lagrangian with which the $V_{\text{low }k}$ RG flow is to be performed can be put in the concise form $\frac{m_N^*}{m_N} \approx \frac{m_\sigma^*}{m_\sigma} \approx y_V \frac{m_V^*}{m_V} \approx \frac{\langle \chi \rangle^*}{\langle \chi \rangle}$ with $y_V = (\frac{g_V^*}{g_V})^{-1}$ and $V = (\rho, \omega)$. Apart from the quantity y_V which is controlled by IDD$_{\text{matter}}$, the scaling of all light-quark hadrons in nuclear dynamics is dictated by IDD$_{\text{pNG}}$ representing the locking of chiral and scale symmetries.

With no unknown parameters, the properties of nuclear matter are well described by the $V_{\text{low }k}$ RG approach up to the equilibrium density n_0 and are argued to be reliable in R-I up to the topology change density $n_{1/2} \approx 2n_0$. In R-II, in contrast, due to the paucity of both theoretical and experimental input, it is found to be difficult to pin down reliably the parameters of the bare Lagrangian. However relying on theoretical arguments based on the vector manifestation property of the ρ vector meson and the pseudo-Nambu-Goldstone nature of π and σ, we were able to fix almost all except for the y_ω for the ω-NN coupling due to the apparent breakdown of U(2) symmetry at high density. Assuming that the Fermi-liquid structure, known to be valid in the vicinity of nuclear matter density, continues to be applicable in R-II up to the range of densities involved in compact stars, say, $\sim$(5–6)n_0, we were able to satisfactorily confront the properties of the recently observed massive neutron stars. We admit that were the Fermi-liquid structure broken in the density regime concerned—which cannot be excluded in the vicinity of the possible IR fixed point [54], our results could not be trusted.

To summarize what we have found, the topology change that takes place in the skyrmion description of nucleons, incorporated into bsHLS Lagrangian, has a dramatic effect in the density regime $n > n_{1/2} \sim 2n_0$ on the EoS of compact-star matter. It affects the bare parameters of the effective Lagrangian due to the existence of both the VM fixed point of the ρ meson and the IR fixed point associated with the dilaton:

(i) It makes the nuclear tensor forces for $n \gtrsim n_{1/2}$ predominantly controlled by the pseudo-NG pion, with the competing ρ tensor strongly suppressed, and induces a shift at $n_{1/2}$ from soft, as needed in heavy-ion collisions [57], to hard in the EoS, especially the symmetry energy, as needed for massive neutron stars.

(iii) The changeover from skyrmion matter to half-skyrmion matter observed in the skyrmion-crystal description resembles, uncannily, the smooth transition at $n \sim (2–3)n_0$ from hadronic matter to strongly coupled quark matter recently discussed [55,58,59]. In particular the half-skyrmion phase could be identified with the quarkyonic phase of [59].

(iii) The U(2) symmetry for (ρ, ω) which holds fairly well in the vacuum—and presumably in R-I—must

be broken down at high density in R-II. Otherwise there will be inconsistency with the properties of the observed massive stars.

(iv) The topology change with the consequent IDD parameter changes makes the ω repulsion dominate over the σ attraction in R-II. This could potentially prevent the hyperons from appearing at a density $n \lesssim 6n_0$, thus resolving the "hyperon problem." This could also be interpreted as the mechanism that accounts for the observed small binding energy—an order of magnitude small relative to QCD scale—for nuclei and nuclear matter, leading effectively to a BPS structure of baryonic matter discussed in Ref. [1], seemingly at odds with QCD in the large N_c limit. The same mechanism could prevent kaon condensations in the same range of density as that of hyperons but this requires further studies.

(v) What in our view is the most significant among our observations is the origin of proton mass as opposed to that of quark mass. The prediction of CT theory that the proton mass is dominantly gluonic, nonvanishing as the quark condensate goes to zero, and hence chirally invariant, is, albeit indirectly, supported by the results of this calculation. This suggests that the mechanism for the proton mass generation lies outside of the standard paradigm based on spontaneous breaking of chiral symmetry. This feature is supported by skyrmion crystal models as well as parity-doubling baryon models.

Finally we should mention a fundamental issue related to the scale-chiral symmetry considered and its potential generalization. In considering the scaling properties of baryons and mesons, we have implemented only the vector manifestation of ρ which brings (in the chiral limit) π and ρ into a zero mass multiplet. On the other hand, the scale-chiral symmetry considered in this paper implies the joining (in the chiral and scale limit) of π and dilaton σ into a zero-mass multiplet. The two could correspond to the same zero-mass multiplet. Together with the a_1, they could then constitute the multiplet figuring in Weinberg's mended symmetries [60]. As discussed in Ref. [1], a possible scenario could be that π, σ, ρ, and a_1 all come together in a massless multiplet at the chiral-scale restoration density. In the scaling behavior discussed above, a_1, not considered explicitly in this paper, could plausibly join π and ρ [61] but there is no indication for the σ dropping to zero within the range of densities involved. How and where they all tend to the mended symmetry limit, if such a limit exists, is not clear. This possibility contrasts with the supersymmetric QCD scenario (for ρ) of [5].

ACKNOWLEDGMENTS
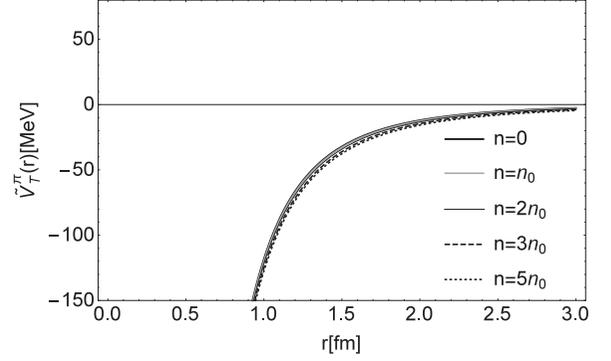
FIG. 12. $\tilde{V}_T^\pi(r) \equiv V_T^\pi(r)(\tau_1 \tau_2 S_{12})^{-1}$ with $n_{1/2} = 2n_0$.

APPENDIX A: DENSITY INDEPENDENCE OF THE PION TENSOR FORCE

In Sec. IV B—and in all previous works on tensor forces implemented with IDDs—the density dependence of the pion tensor force was ignored, arguing that it is protected by chiral symmetry. Here we show explicitly that the argument is correct.

As shown in Sec. IV B, the pion tensor depends on density only via m_π^*. To impose the scaling of m_π^* consistently, we take in R-I

$$\frac{m_\pi^*}{m_\pi} = \Phi_I^{1/2}(n) \approx \left(\frac{1}{1 + 0.13 * n/n_0}\right)^{1/2}. \quad \text{(A1)}$$

In R-II, the pion mass must drop fast since the bilinear quark condensate tends to zero, so it is reasonable to take it to decease
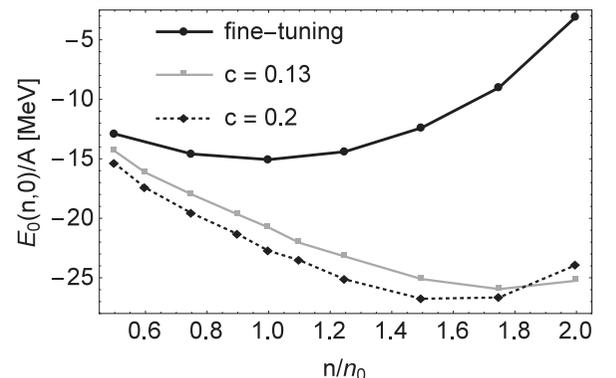
FIG. 13. Ground-state energy $E_0(n,0)$ of symmetric nuclear matter with one parameter c_I in the range 0.13–0.2.
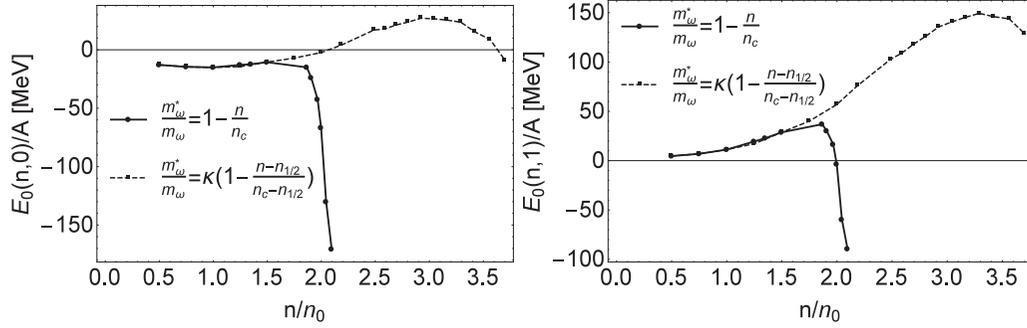
FIG. 14. Ground-state energy $E_0(n,0)$ of symmetric nuclear matter (left panel) and neutron matter (right panel) with U(2) symmetry for (ρ,ω).

rapidly and vanishing at the VM fixed point. Thus

$$\frac{m_\pi^{*2}}{m_\pi^2} \approx \frac{1}{f_{0\pi}^2 \kappa^2 m_\pi^2} \sum_{n>1} c_n \langle (\bar{q}q)^n \rangle \sim \left(1 - 0.15 * \frac{n}{n_0}\right)^2. \quad \text{(A2)}$$

The result is shown in Fig. 12. We find that the pion tensor is more or less independent of density both in R-I and in R-II although m_π^* depends on density, where we used Fermi-Dirac distribution function as

$$\frac{m_\pi^*}{m_\pi} = \left(\frac{1}{1 + 0.13 * n/n_0}\right)^{1/2} \frac{1}{1 + \exp\left(\frac{n-n_{1/2}}{0.05n_0}\right)}$$

$$+ \left(1 - 0.15 * \frac{n}{n_0}\right) \frac{1}{1 + \exp\left(-\frac{n-n_{1/2}}{0.05n_0}\right)} \quad \text{(A3)}$$

to make m_π^* continuous at $n = n_{1/2}$. Thus taking the pion tensor density-independent in doing the $V_{\text{low }K}$ calculation in Sec. VI is justified.

APPENDIX B: ONE-PARAMETER DESCRIPTION OF R-I

In Sec. VI, we have shown with a small fine-tuning for the constant c_I consistent with the expected relation $c_I(N,\sigma) < c_I(\rho,\omega)$ that nuclear matter can be reproduced well within the empirical error bars. Suppose one sticks to the one-c_I strategy and asks how well nuclear matter can be reproduced. This has been checked for the range of $c_I = (0.13-0.20)$. We see from Fig. 13 that taking a universal scaling parameter within a narrow range of the c_I values fails to reproduce Nature. This may be due to different $1/N_c$ corrections contributing to the c_I coefficients and clearly indicates the extremely fine-tuned nature of the ground-state property of nuclear matter.

APPENDIX C: FATE OF HIDDEN LOCAL U(2) SYMMETRY FOR (ρ,ω) IN REGION II

In Sec. IV A 2, while local U(2) symmetry was assumed to hold in Region I (i.e., $n \leqslant n_{1/2}$), we suggested that it should break down in R-II. There is no known theoretical

argument either for or against this suggestion. Here we show an unequivocal indication from Nature that at least *within the present framework* the symmetry should indeed break down in the density regime $n \gtrsim 2n_0$. The argument is based on the assumption that there is a vector manifestation (VM) fixed point $n_{VM} \approx n_c \sim (6-7)n_0$ at which the ρ mass vanishes (in the chiral limit).

Now let us suppose that the U(2) symmetry holds in R-II. This would imply that near the chiral restoration point, the VM would hold for both ρ and ω. We consider two possibilities: One scaling with the same slope in R-II and approaching the same point of VM,

$$m_\omega^*/m_\omega \approx g_\omega^*/g_\omega \approx g^*/g \approx (1 - n/n_c), \quad \text{(C1)}$$

and the other approaching the VM fixed point with different slopes,

$$m_\omega^*/m_\omega \approx \kappa \, g_\omega^*/g_\omega \approx \kappa \left(1 - \frac{n - n_{1/2}}{n_c - n_{1/2}}\right). \quad \text{(C2)}$$

A drastic simplification is made on both and one should be cautious on the interpretation. Nonetheless, the qualitative feature can be taken robust. With all other parameters of Sec. VI fixed the same, the ground-state energy of symmetric nuclear matter comes out as in Fig. 14.

One finds that both the symmetric matter and neutron matter become unstable at $n \sim 2n_0$ for (C1) and $n \sim 3n_0$ for (C2). This signals the breakdown. It takes place principally because the movement toward the VM fixed point softens the repulsion due to the ω exchange, the dropping ω-nucleon coupling "winning over" the increase in repulsion coming from the dropping mass. This makes the dilaton-exchange attraction take over, leading to the collapse. Although the oversimplified linear d-scaling must bring about a precocious breakdown, this result indicates unequivocally that local U(2) symmetry is untenable at high densities above $n_{1/2}$. We take this as a signal from compact stars that the hidden U(2) gauge symmetry must be, perhaps badly, broken at high density.

---

[1] H. K. Lee, W.-G. Paeng, and M. Rho, Scalar pseudo-Nambu-Goldstone boson in nuclei and dense nuclear matter, Phys. Rev. D **92**, 125033 (2015).

[2] R. J. Crewther and L. C. Tunstall, $\Delta I = 1/2$ rule for kaon decays derived from QCD infrared fixed point, Phys. Rev. D **91**, 034016 (2015).

[3] M. Harada and K. Yamawaki, Hidden local symmetry at loop: A New perspective of composite gauge boson and chiral phase transition, Phys. Rep. **381**, 1 (2003).

[4] H. S. Fukano, S. Matsuzaki, K. Terashi, and K. Yamawaki, Conformal Barrier and Hidden Local Symmetry Constraints: Walking Technirhos in LHC Diboson Channels, Nucl. Phys. B **904**, 400 (2016); K. Yamawaki, Old Wine in a New Bottle: Technidilaton as the 125 GeV Higgs – Dedicated to the late Professor Yoichiro Nambu, arXiv:1511.06883.

[5] Z. Komargodski, Vector mesons and an Interpretation of Seiberg duality, J. High Energy Phys. 02 (2011) 019.

[6] Y. L. Ma, M. Harada, H. K. Lee, Y. Oh, B. Y. Park, and M. Rho, Dense baryonic matter in conformally-compensated hidden local symmetry: Vector manifestation and chiral symmetry restoration, Phys. Rev. D **90**, 034015 (2014).

[7] S. K. Bogner, T. T. S. Kuo, and A. Schwenk, Model independent low momentum nucleon interaction from phase shift equivalence, Phys. Rep. **386**, 1 (2003).

[8] S. K. Bogner, T. T. S. Kuo, A. Schwenk, D. R. Entem, and R. Machleidt, Towards a model independent low momentum nucleon nucleon interaction, Phys. Lett. B **576**, 265 (2003).

[9] G. E. Brown and M. Rho, Double decimation and sliding vacua in the nuclear many body system, Phys. Rep. **396**, 1 (2004).

[10] H. Dong, T. T. S. Kuo, H. K. Lee, R. Machleidt, and M. Rho, Half-skyrmions and the equation of state for compact-star matter, Phys. Rev. C **87**, 054332 (2013).

[11] J. W. Holt, G. E. Brown, J. D. Holt, and T. T. S. Kuo, Nuclear matter with Brown-Rho-scaled Fermi liquid interactions, Nucl. Phys. A **785**, 322 (2007).

[12] See *The Multifaceted Skyrmion*, 2nd ed., edited by M. Rho and I. Zahed (World Scientific, Singapore, 2016).

[13] R. A. Battye, N. S. Manton, and P. M. Sutcliffe, in *The Multifaceted Skyrmion* (Ref. [12]).

[14] H. J. Lee, B. Y. Park, M. Rho, and V. Vento, The pion velocity in dense skyrmion matter, Nucl. Phys. A **741**, 161 (2004).

[15] T. H. R. Skyrme, A unified field theory of mesons and baryons, Nucl. Phys. **31**, 556 (1962).

[16] H. K. Lee, B. Y. Park, and M. Rho, Half-skyrmions, tensor forces and symmetry energy in cold dense matter, Phys. Rev. C **83**, 025206 (2011); Erratum: Half-Skyrmions, tensor forces, and symmetry energy in cold dense matter [Phys. Rev. C 83, 025206 (2011)], **84**, 059902(E) (2011).

[17] I. Vidana, A. Polls, and C. Providencia, Nuclear symmetry energy and the role of the tensor force, Phys. Rev. C **84**, 062801 (2011).

[18] J. W. Holt, G. E. Brown, T. T. S. Kuo, J. D. Holt, and R. Machleidt, Shell Model Description of the ^{14}C Dating β Decay with Brown-Rho-Scaled *NN* Interactions, Phys. Rev. Lett. **100**, 062501 (2008).

[19] J. W. Holt, M. Rho, and W. Weise, Chiral symmetry and effective field theories for hadronic, nuclear and stellar matter, Phys. Rept. **621**, 2 (2016).

[20] M. Harada, Y. Kim, M. Rho, and C. Sasaki, The Pion velocity at chiral restoration and the vector manifestation, Nucl. Phys. A **730**, 379 (2004); The Vector and axial vector susceptibilities and effective degrees of freedom in the vector manifestation, *ibid.* **727**, 437 (2003).

[21] T. Buchheim, B. Kampfer, and T. Hilger, Algebraic vacuum limits of QCD condensates from in-medium projections of Lorentz tensors, J. Phys. G **43**, 055105 (2016).

[22] D. T. Son and M. A. Stephanov, Pion Propagation Near the QCD Chiral Phase Transition, Phys. Rev. Lett. **88**, 202302 (2002).

[23] W. G. Paeng, H. K. Lee, M. Rho, and C. Sasaki, Interplay between ω-nucleon interaction and nucleon mass in dense baryonic matter, Phys. Rev. D **88**, 105019 (2013).

[24] M. Rho, Quenching of axial-vector coupling constant in beta-decay and pion-nucleus optical potential, Nucl. Phys. A **231**, 493 (1974).

[25] G. E. Brown and M. Rho, From chiral mean field to Walecka mean field and kaon condensation, Nucl. Phys. A **596**, 503 (1996).

[26] R. Shankar, Renormalization group approach to interacting fermions, Rev. Mod. Phys. **66**, 129 (1994).

[27] C. Xu and B. A. Li, Understanding the major uncertainties in the nuclear symmetry energy at suprasaturation densities, Phys. Rev. C **81**, 064612 (2010).

[28] G. E. Brown, C. H. Lee, H. J. Park, and M. Rho, Study of Strangeness Condensation by Expanding About the Fixed Point of the Harada-Yamawaki Vector Manifestation, Phys. Rev. Lett. **96**, 062303 (2006).

[29] R. Machleidt, The Meson theory of nuclear forces and nuclear structure, Adv. Nucl. Phys. **19**, 189 (1989).

[30] I. I. Kogan, A. Kovner, and M. Shifman, Chiral symmetry breaking without bilinear condensates, unbroken axial Z(N) symmetry, and exact QCD inequalities, Phys. Rev. D **59**, 016001 (1999); Y. Watanabe, K. Fukushima, and T. Hatsuda, Order parameters with higher dimensionful composite fields, Prog. Theor. Phys. **111**, 967 (2004); M. Harada, C. Sasaki, and S. Takemoto, Enhancement of quark number susceptibility with an alternative pattern of chiral symmetry breaking in dense matter, Phys. Rev. D **81**, 016009 (2010).

[31] M. Harada, T. Kugo, and K. Yamawaki, Proving the Low-Energy Theorem of Hidden Local Symmetry, Phys. Rev. Lett. **71**, 1299 (1993).

[32] C. Sasaki, H. K. Lee, W. G. Paeng, and M. Rho, Conformal anomaly and the vector coupling in dense matter, Phys. Rev. D **84**, 034011 (2011); W. G. Paeng, H. K. Lee, M. Rho, and C. Sasaki, Dilaton-limit fixed point in hidden local symmetric parity doublet model, *ibid.* **85**, 054022 (2012).

[33] G. E. Brown and R. Machleidt, Strength of the ρ meson coupling to nucleons, Phys. Rev. C **50**, 1731 (1994).

[34] H. K. Lee and M. Rho, Topology change and tensor forces for the EoS of dense baryonic matter, Eur. Phys. J. A **50**, 14 (2014).

[35] R. Machleidt in *Computational Nuclear Physics 2–Nuclear Reactions*, edited by K. Langanke, J. A. Maruhn, and S. E. Koonin (Springer, New York, 1993).

[36] H. Dong, T. T. S. Kuo, and R. Machleidt, Low-momentum interactions with Brown-Rho-Ericson scalings and the density dependence of the nuclear symmetry energy, Phys. Rev. C **83**, 054002 (2011).

[37] L.-W. Siu, J. W. Holt, T. T. S. Kuo, and G. E. Brown, Low-momentum NN interactions and all-order summation of ring diagrams of symmetric nuclear matter, Phys. Rev. C **79**, 054004 (2009).

[38] H. Dong, T. T. S. Kuo, and R. Machleidt, Neutron star and beta-stable ring-diagram equation of state with Brown-Rho scaling, Phys. Rev. C **80**, 065803 (2009).

[39] L.-W. Siu, T. T. S. Kuo, and R. Machleidt, Low-momentum ring diagrams of neutron matter at and near the unitary limit, Phys. Rev. C **77**, 034001 (2008).

[40] H. Dong, L.-W. Siu, T. T. S. Kuo, and R. Machleidt, Unitarity potentials and neutron matter at the unitary limit, Phys. Rev. C **81**, 034003 (2010).

[41] B. Friman and M. Rho, From chiral Lagrangians to Landau Fermi liquid theory of nuclear matter, Nucl. Phys. A **606**, 303 (1996).

[42] P. Danielewicz, R. Lacey, and W. G. Lynch, Determination of the equation of state of dense matter, Science **298**, 1592 (2002).

[43] B. A. Li and L. W. Chen, Nucleon-nucleon cross sections in neutron-rich matter and isospin transport in heavy-ion reactions at intermediate energies, Phys. Rev. C **72**, 064611 (2005).

[44] M. B. Tsang, Y. Zhang, P. Danielewicz, M. Famiano, Z. Li, W. G. Lynch, and A. W. Steiner, Constraints on the Density Dependence of the Symmetry Energy, Phys. Rev. Lett. **102**, 122701 (2009).

[45] J. M. Lattimer and Y. Lim, Constraining the Symmetry Parameters of the Nuclear Interaction, Astrophys. J. **771**, 51 (2013).

[46] J. Antoniadis *et al.*, A massive pulsar in a compact relativistic binary, Science **340**, 6131 (2013).

[47] J. M. Lattimer and B. F. Schutz, Constraining the equation of state with moment of inertia measurements, Astrophys. J. **629**, 979 (2005).

[48] N. K. Glendenning, The hyperon composition of neutron stars, Phys. Lett. B **114**, 392 (1982).

[49] P. F. Bedaque and A. W. Steiner, Hypernuclei and the hyperon problem in neutron stars, Phys. Rev. C **92**, 025803 (2015).

[50] H. K. Lee and M. Rho, Hyperons and condensed kaons in compact stars, arXiv:1301.0067.

[51] C. G. Callan, Jr. and I. R. Klebanov, Bound state approach to strangeness in the Skyrme model, Nucl. Phys. B **262**, 365 (1985).

[52] H. Guo, R. Zhou, B. Liu, X.-G. Li, and Y.-X. Liu, In-medium kaon and antikaon production and antikaon condensation in neutron star matter, Astrophys. J. **622**, 549 (2005).

[53] V. R. Pandharipande, C. J. Pethick, and V. Thorsson, Kaon Energies in Dense Matter, Phys. Rev. Lett. **75**, 4567 (1995).

[54] W. G. Paeng and M. Rho, Kaon condensation in baryonic Fermi liquid at high density, Phys. Rev. C **91**, 015801 (2015).

[55] T. Kojo, P. D. Powell, Y. Song, and G. Baym, Phenomenological QCD equation of state for massive neutron stars, Phys. Rev. D **91**, 045003 (2015).

[56] K. Kim, H. K. Lee, and M. Rho, Triple layered compact star with strange quark matter, Int. J. Mod. Phys. Conf. Ser. **10**, 123 (2012).

[57] L. Tolos, I. Sagert, D. Chatterjee, J. Schaffner-Bielich, and C. Sturm, Implications for compact stars of a soft nuclear equation of state from heavy-ion data, PoS **NICXII**, 036 (2012).

[58] K. Masuda, T. Hatsuda, and T. Takatsuka, Hyperon puzzle, hadron-quark crossover and massive neutron stars, Eur. Phys. J. A **52**, 65 (2016).

[59] K. Fukushima and T. Kojo, The quarkyonic star, Astrophys. J. **817**, 180 (2016).

[60] S. Weinberg, Mended Symmetries, Phys. Rev. Lett. **65**, 1177 (1990); *Unbreaking Symmetries, Salamfestschrift*, edited by A. Ali, J. Ellis and S. Randjbar-Daemi (World Scientific, Singapore, 1994).

[61] M. Harada and C. Sasaki, Dropping ρ and a_1 meson masses at chiral phase transition in the generalized hidden local symmetry, Phys. Rev. D **73**, 036001 (2006); Y. Hidaka, O. Morimatsu, and M. Ohtani, Renormalization group equations in a model of generalized hidden local symmetry and restoration of chiral symmetry, *ibid.* **73**, 036004 (2006).